Marine Ecosystems of the North Pacific Ocean 2003-2008

McKinnell, S.M. and Dagg, M.J. [Eds.] 2010.
Marine Ecosystems of the North Pacific Ocean, 2003-2008.
PICES Special Publication 4, 393 p.

PICES Special Publication Number 4

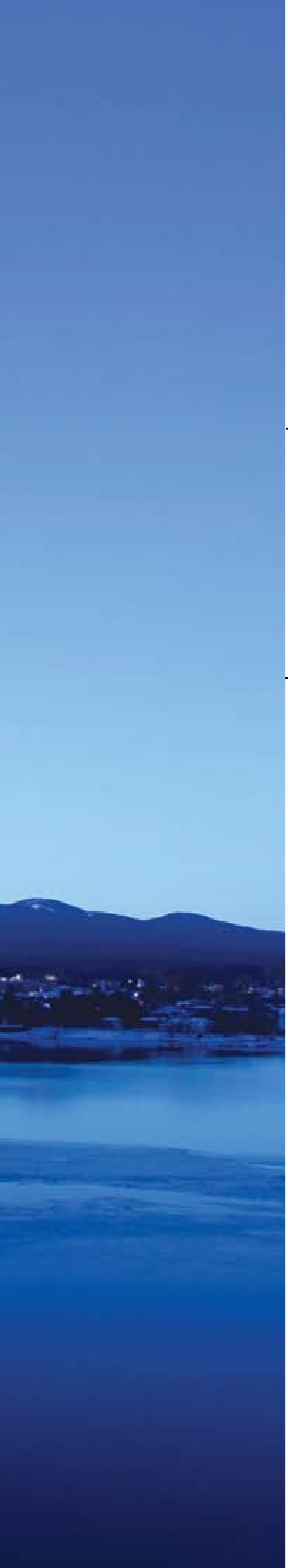

Kuroshio

lead author

Hiroya Sugisaki

National Research Institute of Fisheries Science
Fisheries Research Agency
Yokohama, Japan

Citation:

Sugisaki, H., Nonaka, M., Ishizaki, S., Hidaka, K., Kameda, T., Hirota, Y., Oozeki, Y., Kubota, H., Takasuka, A. 2010. Status and trends of the Kuroshio region, 2003-2008, pp. 330-359 In S.M. McKinnell and M.J. Dagg [Eds.] Marine Ecosystems of the North Pacific Ocean, 2003-2008. PICES Special Publication 4, 393 p.

highlights

- The strength of the Kuroshio is related to the magnitude of the Aleutian Low with a 5-year lag time. Weakening of the Aleutian Low in recent years suggests the Kuroshio should be weakening, and data indicate transport has been gradually decreasing since 2006.

- From 2003 to 2007, large anomalies and trends were not observed in the physical and biological properties of the Kuroshio. Some annual variation of atmospheric and oceanic conditions was observed. The Large-Meander pattern of the Kuroshio was observed during late 2004 and early 2005.

- Low nutrient concentrations and low seasonal variations of chlorophyll concentration and copepod biomass were observed after the Large-Meander year. During meander years, the species composition of diatoms was different from that of non-Large-Meander years. The meander may cause a change in species composition of the plankton community. Some clear ecological differences were observed before and after the large meander. The meander may cause an abrupt ecological change.

- Since physical conditions and biological production have not changed or fluctuated strongly except for the meander period during late 2004 and early 2005, the survival of pelagic fish larvae is thought to have been relatively stable during the focus period. This stability may have been the cause of low recruitment of Japanese sardine and jack mackerel that, in turn, led to continued low abundance from 2003 to 2007. On the other hand, Japanese anchovy were abundant and widespread during these years. High temperature conditions on land and in coastal areas in recent years may favor anchovy rather than sardine (Takasuka et al. 2008).

Introduction

Originating in the North Equatorial Current, the Kuroshio is the western boundary warm current in the North Pacific (Fig. KU-1). It flows along the south side of the Japanese Archipelago, crossing three shallow ridges – one east of Taiwan, through Tokara Strait, and across the Izu-Ogasawara ridges. The width of the Kuroshio is about 100 km and a current speed is 1-2 $m \cdot s^{-1}$. The depth of the current axis is usually >500 m and the transport volume is about 50 Sv. Large amounts of water are exchanged with several stable eddies in the region such as the large warm eddy to the south of Shikoku Island. The Kuroshio feeds the Kuroshio Extension off eastern Japan where it forms a broad Mixed Water Region to the north of the Kuroshio Extension. Usually there is a large meander east of Honshu Island which frequently ejects large warm-core rings into the Mixed Water Region. The high temperature and high salinity of Kuroshio water brings a high diversity of tropical marine life northward (to ~40°N) to the coastal area of the Japanese archipelago and off eastern Japan. Many species of invertebrates (e.g. corals) and vertebrates (e.g. butterfly fishes) from more southern latitudes have been recorded near the south coast of Japan but most of them cannot survive and reproduce because of the cold winter water temperatures in the coastal area and the low nutrient concentrations of the Kuroshio. However, this indicates that the Kuroshio can support, at least temporarily, these species in more northern areas.

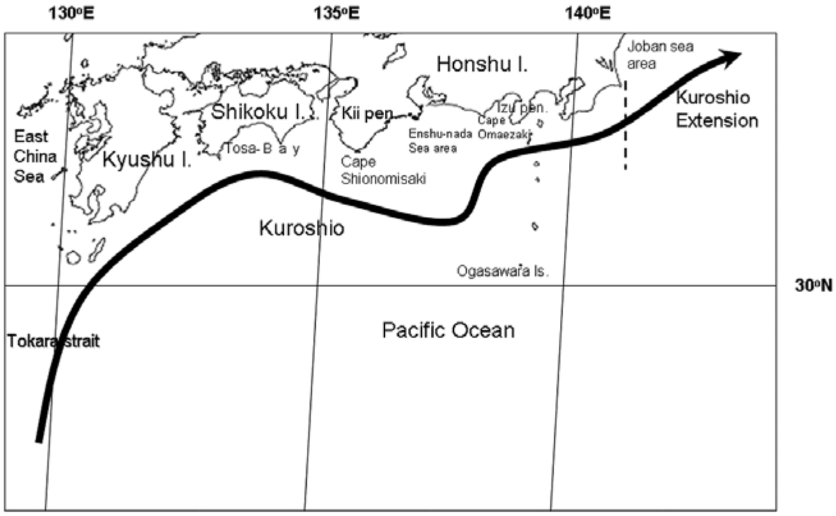

[Figure KU-1] The typical path of the Kuroshio and Kuroshio Extension and geographical names used in this chapter.

Since nutrient concentrations and biological production in the Kuroshio are much lower than in the cold western boundary current (Oyashio) to the north, commercial fishing in the Kuroshio is small compared to the Oyashio area. Nevertheless, the Kuroshio is a major spawning area for many species of pelagic fishes such as Japanese sardine (*Sardinops melanostictus*) and Pacific saury (*Cololabis saira*) that have their nursery and feeding grounds in the Oyashio area. Therefore, the environment of the Kuroshio affects the spawning conditions and survival rate of early life stages of many species of pelagic fish. These species exhibit high amplitude variation in stock size and community composition. The mechanisms of stock size variation and species alternation are thought to be related to survival of early life stages. Therefore, environmental change in the Kuroshio region affects the broader ecosystem around Japan (both the Kuroshio and Oyashio oceanic areas and the coastal area of the Japan trench). The status of the Kuroshio is important for understanding both global change and fisheries conditions of the North Pacific. This chapter contains a review of the status and trends of the Kuroshio Region from 2003-2008, hereafter termed the *focus period*.

2.0 Atmosphere *(Nonaka)*

2.1 Sea surface wind field

2.1.1 Wind and Kuroshio transport

Figure KU-2 shows the mean wintertime sea level pressure (SLP) and surface wind fields based on the NCEP/NCAR reanalysis data (Kalnay et al. 1996). The Aleutian low pressure region, centered near 50°N 180°E, is responsible for northwesterly and westerly winds that blow over the Kuroshio and Kuroshio Extension regions, respectively. The combination of easterly trade winds to the south and westerly winds over the mid-latitude North Pacific induce negative (anti-cyclonic) wind stress curl to the south that drives the subtropical gyre. The Kuroshio forms the western boundary of the subtropical gyre in the North Pacific. Deepening of the Aleutian Low can strengthen the current by accelerating flow within the gyre. Transport of the Kuroshio at 137°E has been monitored by the Japan Meteorological Agency (JMA) twice per year since 1972 (Fig. KU-8). These data reveal interannual and decadal variations, and it has been shown that the decadal variations are correlated with the North Pacific Index (NPI) with 5-year lags (Hanawa and Kamada 2001; Yasuda and

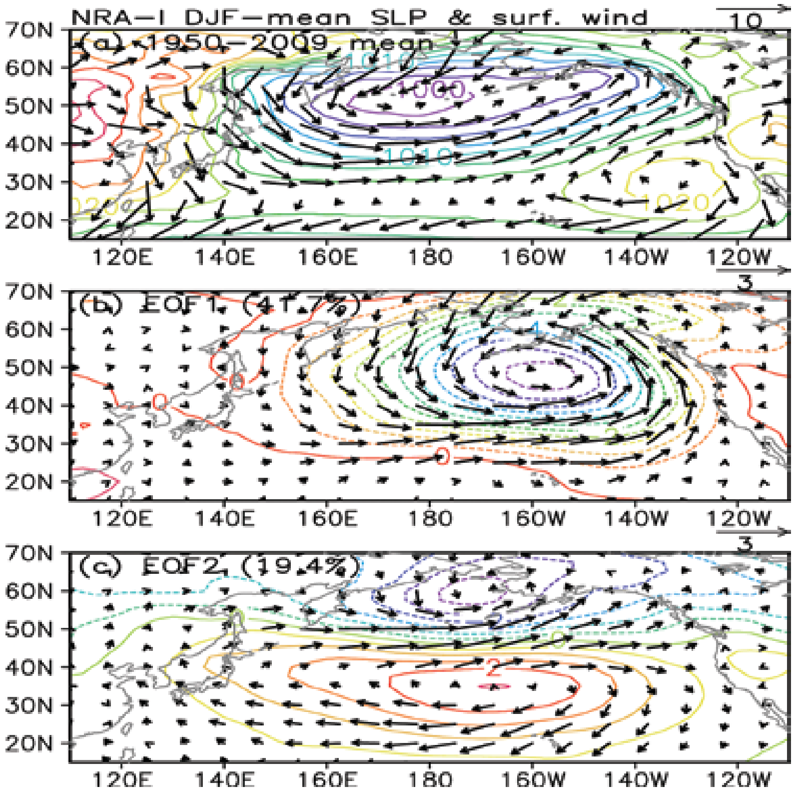

[Figure KU-2] (a) 1950-2009 mean wintertime (December-February) SLP (contours with intervals of 2.5 hPa) and surface wind vectors. (b, c) Maps for SLP (contours with intervals of 0.5 hPa) and surface wind (vectors) regressed linearly on the (b) PC 1 and (c) PC 2 time series for the EOF analysis conducted for the SLP field in (20°-85°N, 120°E-120°W). The scaling for the vectors (m·s⁻¹) is indicated at the upper-right corner of each panel. All variables are based on the NCEP/NCAR reanalysis monthly mean data.

Kitamura 2003). The NPI is defined as an area-weighted mean SLP over the region 30°N-65°N, 160°E-140°W (Trenberth and Hurrell 1994) and its variations represent changes in the intensity and extent of the Aleutian Low in winter. The NPI is highly correlated (r = -0.99 for 1950-2009) with the first empirical orthogonal function (EOF) mode for the SLP field that extends from the central to eastern North Pacific (Fig. KU-2b). Although the NPI has tended to be negative since the mid-1990s, it turned positive after 2005 (Figs. KU-4a and KU-4c), indicating the Aleutian Low weakened in recent years. This suggests that the Kuroshio can be expected to weaken in the near future as pointed out at the JMA website* if the relationship between the NPI and the Kuroshio is causal.

2.1.2 Wind and surface air temperature

Comparison of the wind anomaly fields during the focus period with the climatological mean (Fig. KU-3a) suggests that northwesterly winds from the Eurasian continent and accompanying cold advection associated with the East Asian winter monsoon were weaker in this period. In contrast to this, northwesterly winds to the northeast of Japan were intensified and cold anomalies were found there. These patterns were found in 2003, 2004, 2007, and 2008. Especially in 2007, winds from the northwest were weak, as indicated by the relatively strong wind anomalies from the direction generally opposite to that for the mean winds. Warm air temperature anomalies extended southeastward from the Eurasian continent to the Kuroshio Extension region (Fig. KU-3g). In contrast, during 2006, the northwesterly (westerly) winds to the northwest (east) of Japan were intensified (Fig. KU-3f) and cold air temperature anomalies covered the Kuroshio and Kuroshio Extension regions. Honda et al. (2009) suggest that part of this extent of cold air from the Eurasia continent in 2006 was associated with anomalies in large-scale atmospheric circulation caused by a decrease of sea-ice cover in the Arctic Ocean, more specifically, in the Barents and Kara seas, in the preceding summer-to-autumn seasons.

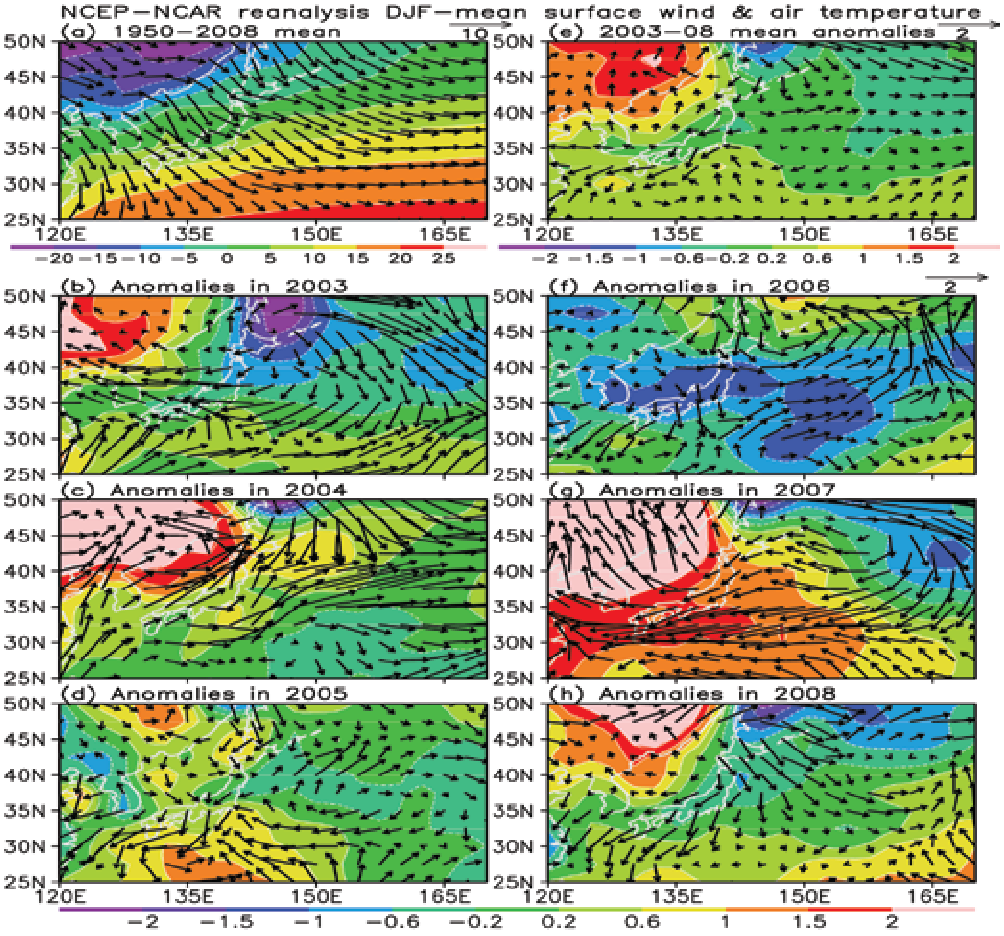

[Figure KU-3] (a) 1950-2008 mean wintertime (December-February) surface air temperature and surface wind. (e) 2003-2008 mean anomaly fields of surface air temperature and surface wind from the climatological mean field shown in (a). Panels(b-d, f-h) are the same as (b) but for each winter from 2003 to 2008 as indicated above each panel. Shadings show surface air temperature and its anomalies (°C) as indicated below each panel for (a) and (e), and below all panels for (b-d, f-h). The scaling for the wind vectors (m·s⁻¹) is indicated at the upper-right corner of each panel for (a) and (e), and at the upper-right of panel (f) for (b-d, f-h). All variables are based on the NCEP/NCAR reanalysis monthly mean data.

---

* http://www.data.kishou.go.jp/kaiyou/shindan/b.2/kuroshio-slow/kuroshio_flow.html

2.1.3 Wind and the Kuroshio Extension

The strength and latitude of the Kuroshio Extension Current (KEC) varies decadally (Qiu and Chen 2005; Taguchi et al. 2007). Sea surface height observations since the 1990s have shown that the KEC intensifies when its axis shifts northward (Qiu and Chen 2005), although a 50-year-long hindcast simulation by an eddy-resolving ocean general circulation model suggests that this relation was not clear before the 1980s (e.g. Taguchi et al. 2007; Nonaka et al. 2006). The meridional shift of the KEC may be caused by atmospheric changes over the whole North Pacific like the first EOF mode of SLP (Seager et al. 2001; Miller et al. 1998; Deser et al. 1999). In contrast to this, the aforementioned hindcast simulation result has found that the KEC tends to intensify following central North Pacific wind variations associated with the North Pacific Oscillation (NPO) with a 2.5-year lag, probably through propagation of Rossby waves (Ceballos et al. 2009). The NPO is the second EOF mode of SLP over the North Pacific and has a meridional dipole structure with the opposite signs over Alaska and Hawaii (Fig. KU-2c; Walker and Bliss 1932; Wallace and Gutzler 1981). Meanwhile the first EOF mode shows a monopole pattern over the northern North Pacific corresponding to the variations of the Aleutian Low (Fig. KU-2b).

The time series of the second EOF mode (Fig. KU-4c, red curve) indicates that the NPO was positive around 1990 and 2000, which corresponded to intensification of the KEC in the early 1990s and 2000s (Taguchi et al. 2007; Qiu and Chen 2005). Although the NPO was negative around 2005, it recovered and was positive for several years after 2006. The positive NPO in recent years is consistent with the recent (2003-2008 mean) properties in the wind anomaly fields in the Kuroshio region (Fig. KU-3e).

2.2 Precipitation

2.2.1 Winter precipitation

Variations in precipitation or in precipitation minus evaporation (P-E) can influence not only surface and subsurface salinity fields (Overland et al. 1999; Lukas 2001), but also the strength of the CO_2 sink at the sea surface (Dore et al. 2003). The long-term mean wintertime precipitation field (Fig. KU-5a) has a local maximum over the KEC around 35˚N associated with the storm-track in the North Pacific (Nakamura et al. 2002, see their Fig. 1). An EOF analysis for wintertime precipitation (and also P-E) indicates that the first EOF mode (Fig. KU-4d, black curve for its principal component, PC1, and Fig. KU-5b) is associated with the

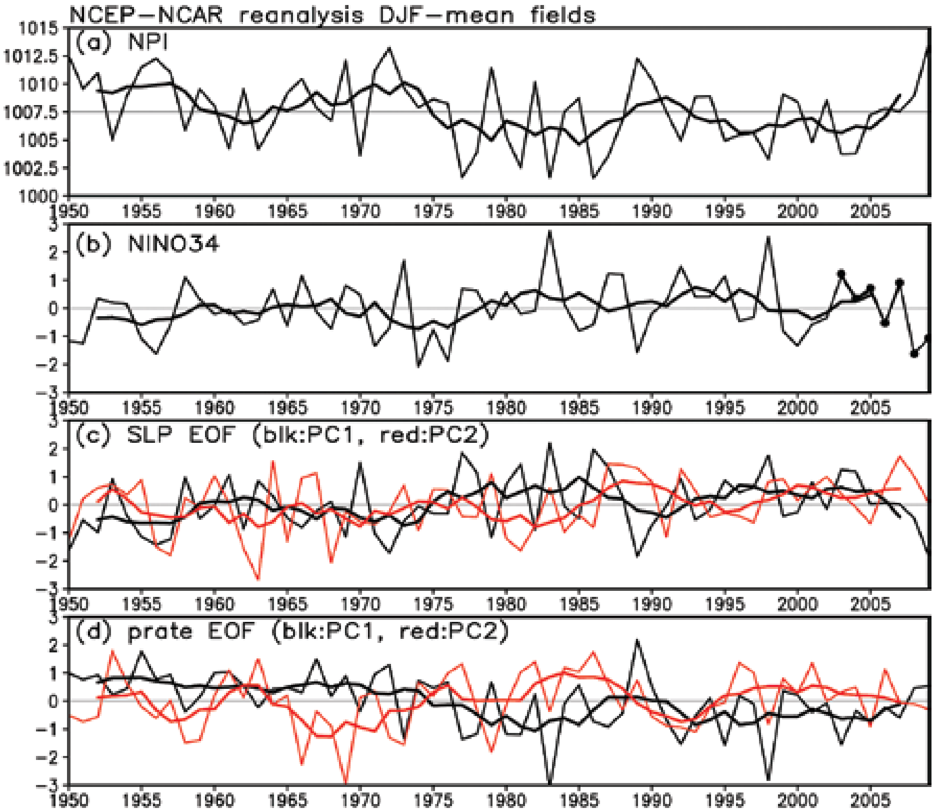

[Figure KU-4] Interannual (thin lines) and 5-year running mean (thick lines) time series of (a) NPI, (b) NINO3.4 index, (c) PC 1 (black) and PC 2 (red) for the EOF analysis of SLP in (20°-85°N, 120°E-120°W), and (d) the same as (c) but for precipitation rate in (8.5°-62°N, 120°E-120°W). All variables are based on the NCEP/NCAR reanalysis monthly mean data except for the SST data for (b) that is based on the HadISST (solid curve for 1950-2004) and AMSR-E SST (solid curve with dots for 2003-2009) compiled at the UK Met office and Remote Sensing Systems, respectively. NINO3.4 index based on AMSR-E SST is plotted just for comparison. Nino3.4 index is defined as area mean SST anomalies in (5°S-5°N, 170°W-120°W).

El Niño/Southern Oscillation (ENSO) (r = -0.78 between NINO3.4 (Fig. KU-4b) and PC1 for 1950-2009) and has a weak signal in the Kuroshio and Kuroshio Extension regions (Lukas 2001, see also his Fig. 2b and Fig. 3).

In contrast to this, the second EOF mode shows three bands of positive and negative precipitation anomalies extending from southwest to northeast, and one of the centers of action extends from south of Japan to the Kuroshio Extension region (Fig. KU-5c; Lukas 2001, see also his Fig. 3), indicating the possible importance of this mode for rainfall variations in the Kuroshio and Kuroshio Extension regions. Similar southwest-to-northeastward band-like structures of precipitation anomalies are also shown in other studies (Overland et al. 1999; Minobe and Nakanowatari 2002; Nakamura et al. 2002; Honda et al. 2005).

The time series corresponding to the second EOF mode (Fig. KU-4d, red curves) is dominated by decadal variation. Focusing on the decadal timescale by applying the 10-30-year band-pass filter, the band-like structure of precipitation anomalies is correlated with the NPI (Minobe and Nakanowatari 2002). This shows that precipitation in the northern part of the North Pacific region varies in association with large-scale SLP anomalies. In the Kuroshio region, stronger rainfall tends to occur with positive NPI anomalies and a weakened Aleutian Low (Minobe and Nakanowatari 2002).

Except for the southernmost of the three bands, the precipitation anomalies in the northern North Pacific are associated with meridional shifts of the storm-track (Nakanowatari and Minobe 2005; Nakamura et al. 2002). Significant decadal-scale variation in latitude of the storm-track and its activity were found at the end of 1980s in conjunction with decadal-scale weakening in the East Asian winter monsoon (Nakamura et al. 2002). From the late-1980s to the mid-1990s, the midwinter Siberian High and the Aleutian Low were weak, and the winter storm-track was located to the north of its climatological position. At the same time, midwinter activity of the storm-track and thus precipitation in the region were enhanced (Nakamura et al. 2002).

As indicated in Figure KU-4d (red curves), the second EOF mode has tended to be positive since the early-1990s in association with a negative NPI and deepened Aleutian Low (Fig. KU-4a). However, in recent years, the Aleutian Low has started to weaken and the East Asian winter monsoon was also weak in 2003-2008 (Fig. KU-3e).

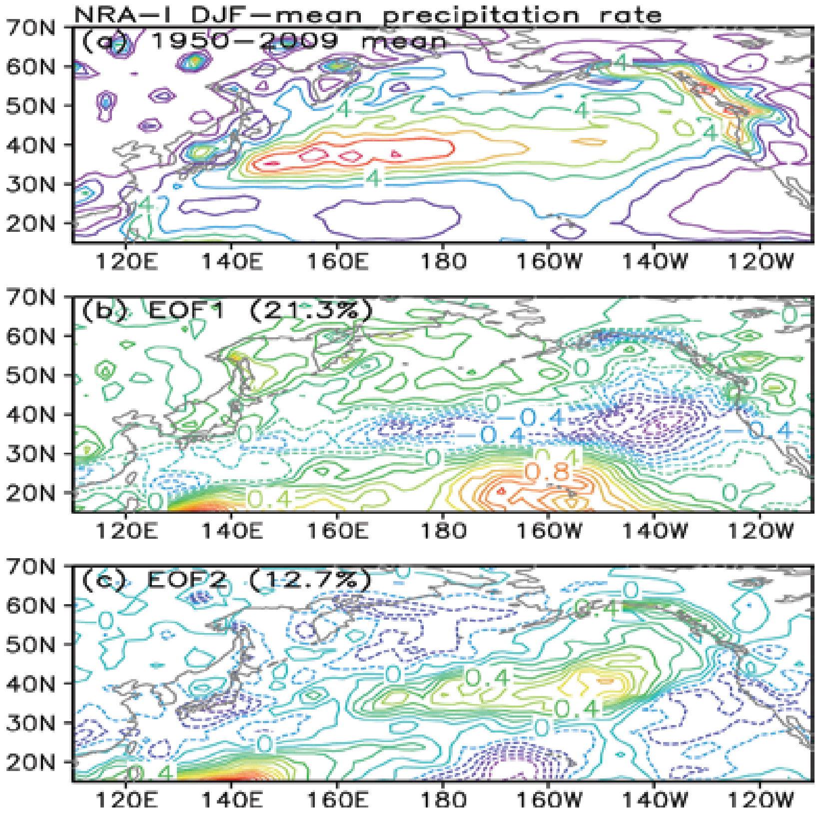

[Figure KU-5] NCEP/NCAR reanalysis wintertime (Dec-Feb) precipitation ratio fields. (a) 1950-2009 mean (contours intervals are 1 mm·d^{-1}). (b, c) Maps for the field (contours intervals are 0.1 mm·d^{-1}) regressed linearly on the (b) PC 1 and (c) PC 2 time series for the EOF analysis conducted for the field in (8.5°-62°N, 120°E-120°W).

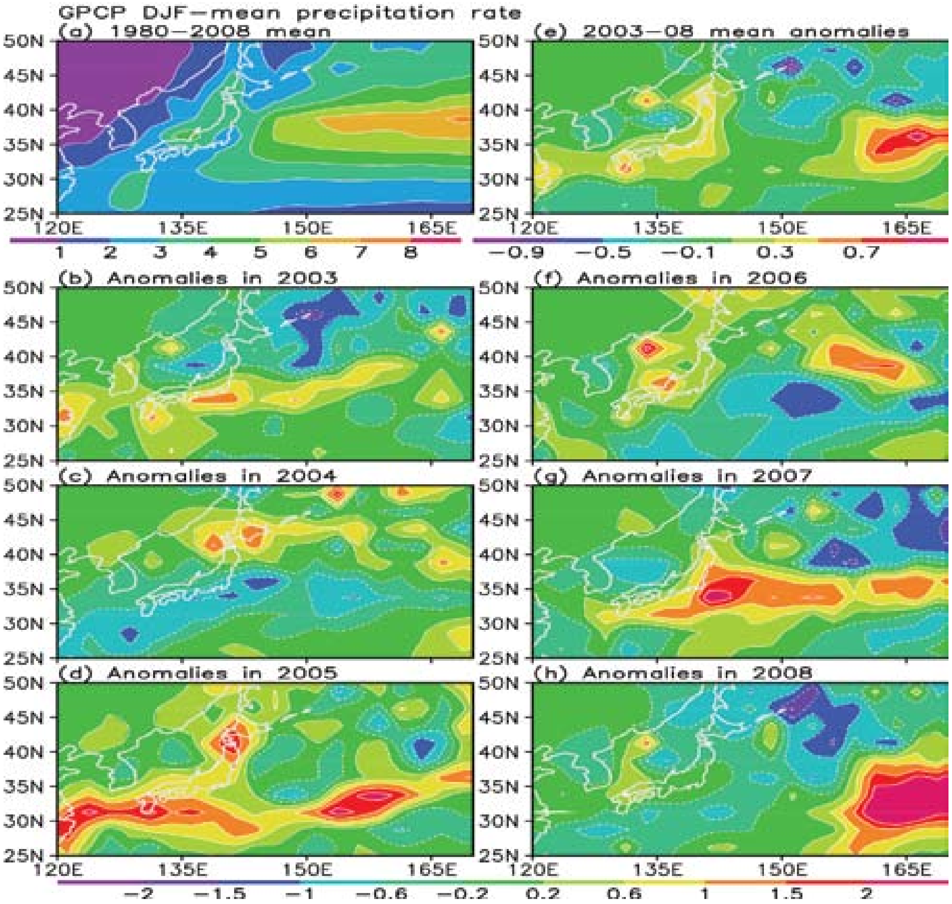

[Figure KU-6] (a) 1980-2008 mean wintertime (Dec-Feb) precipitation rate. (e) 2003-2008 mean anomaly field of precipitation rate from the long-year mean field shown in (a). (b-d, f-h) The same as (b) but for each winter from 2003 to 2008 as indicated above each panel. Shadings show precipitation rate and its anomalies (mm·d⁻¹) as indicated below of each panel for (a) and (e), and below panels (d) and (h). All variables are based on the Global Precipitation Climatology Project (GPCP; Adler et al. 2003) monthly mean data.

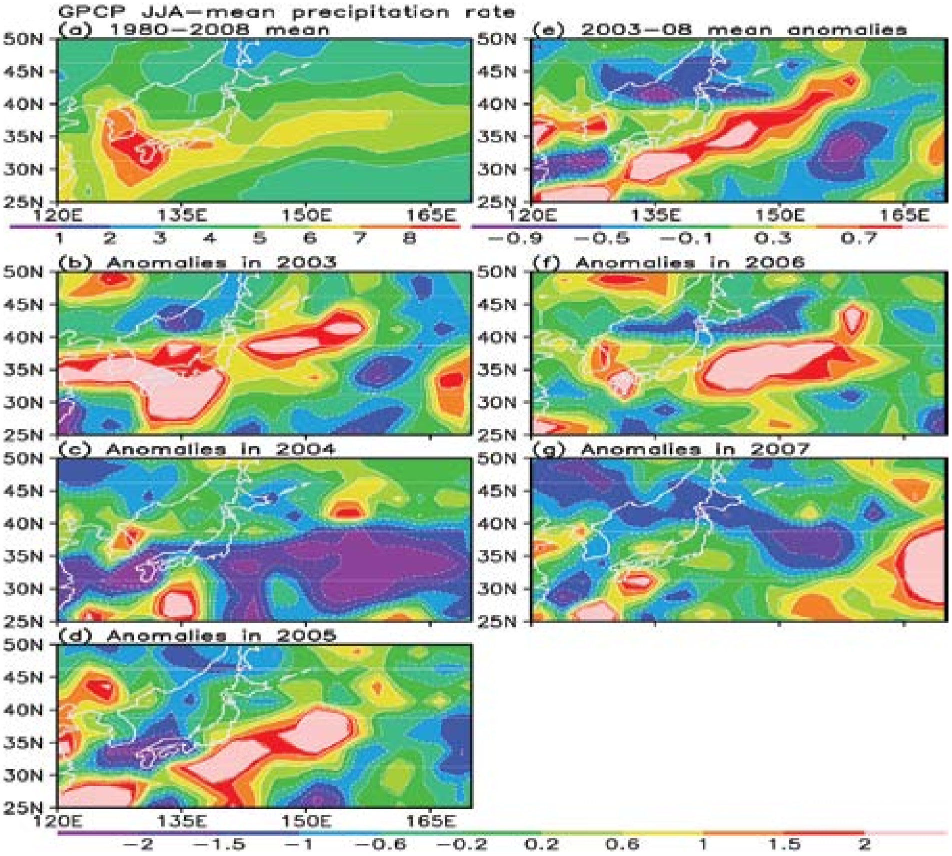

[Figure KU-7] (a) 1980-2007 mean summertime (June-August) precipitation rate. (e) 2003-2007 mean anomaly field of precipitation rate from the long-year mean field shown in (a). (b-d, f-g) The same as (b) but for each winter from 2003 to 2007 as indicated above each panel. Shadings show precipitation rate and its anomalies (mm·d⁻¹) as indicated to the right of each panel for (a) and (e), and below panels (d) and (h). All variables are based on the GPCP monthly mean data.

In association with these changes, precipitation increased around Japan and also around the storm-track to the east of 150°E (Fig. KU-6e). This is consistent with the aforementioned relationships among the East Asian winter monsoon, the Aleutian Low and wintertime precipitation. In the plots for each winter (Fig. KU-6), it is apparent there was large year-to-year variability. Enhanced precipitation was observed in 2003, 2005, and 2007 in the Kuroshio and Kuroshio Extension regions.

2.2.2 Summer precipitation

The climatological mean of summer (June-August) precipitation in the Kuroshio region (Fig. KU-7a) indicates that a high precipitation band (mei-yu/baiu front) extends northeastward from southern China to the western North Pacific through the southern part of Japan. The leading EOF mode of interannual variation in summertime precipitation over the subtropical western North Pacific (20N°-50°N, 100E°-180°E) indicates pronounced centers of action along the mei-yu/baiu front (Lee et al. 2005, their Fig. 1), while the opposite anomalies are found to the south around 10°N-20°N. This mode is closely linked to variations in the East Asian summer monsoon, and tends to occur in the "post-El Niño" summer or the decaying phase of El Niño (Lee et al. 2005; Wang et al. 2008). Heavy rainfall was observed in July 1998 and July 2003 in the Kuroshio and the Kuroshio Extension region following El Niño winters, although heavy rainfall also occurred in 2006 when no El Niño occurred. The 2003-2007 mean anomaly field (Fig. KU-7e) indicates that rainfall in the mei-yu/baiu front was enhanced in 2003, 2005, and 2006 (Fig. KU-7). Enhanced rainfall in the Kuroshio region is associated with relatively continuous warm eastern equatorial Pacific SST during the earlier part of the focus period (Fig. KU-4b). This is consistent with the aforementioned interannual relation between El Niño and the East Asian summer monsoon. The mechanisms that are responsible for the impact of El Niño that peaks in winter on the East Asian summer monsoon have been discussed by Wang et al. (2000) and Xie et al. (2009). The former suggests the importance of air-sea interaction in the western tropical Pacific, and the latter suggests that the prolonged impact is due to a capacitor effect of the Indian Ocean.

3.0 Oceanography

3.1 Hydrography *(Ishizaki)*

The properties of Kuroshio water (e.g. salinity, oxygen concentration) are considerably more stable than those of the Oyashio and Kuroshio-Oyashio transition waters. The annual variation of hydrography in the Kuroshio region is caused mainly by variations in the pathway and transport of Kuroshio water. A time series of the Kuroshio transport along 137°E shows interannual and quasi-decadal variation (Fig. KU-8) corresponding to changes in the wind stress curl in the central North Pacific (Yasuda and Kitamura 2003). During the focus period, transport peaked in 2006 then decreased, but was high again in late 2007 and has decreased since.

The Kuroshio takes three major paths south of Japan: the nearshore and offshore non-Large-Meander paths (nNLM and oNLM), [(1) and (2) in Fig. KU-9], and the typical Large-Meander path (tLM) [(3) in Fig. KU-9] (Kawabe 1995). When it takes the tLM path, the Kuroshio makes a detour around Enshu-nada (between 136°E to 140°E) and its southernmost position is located south of 32°N, while the two NLM paths, which are distinguished by their position over the Izu Ridge (140°E), are close to the coast of Japan (Fig. KU-9). Several experiments for reenacting the path of the Kuroshio using inflow-outflow models (Akimoto et al. 1991, 1997) successfully replicated the three patterns of Kuroshio meanders.

The Kuroshio often took the LM path from 1975-1991 (Fig. KU-10) but it has been taking the NLM path since 1992, except from the second half of 2004 to first half of 2005. The first mode of the EOF of sea surface temperature in the Kuroshio region shows area wide variation. Negative SST anomalies dominated in the Kuroshio region before 1998 (Fig. KU-11a). SST anomalies turned positive in 1998 and continued until 2002. After 2002, distinct trends or events have not been observed in SST in the Kuroshio area. This means that the temperature of the Kuroshio has been moderate and stable since 2002, in contrast to the previous decades.

The second and third EOFs of the SST anomalies have a center of action around Enshu-nada. The second EOF shows negative SST anomalies around Enshu-nada in 1987, 1991, 2001, 2005, corresponding to the period when the Kuroshio took the tLM path (except the Kuroshio took the

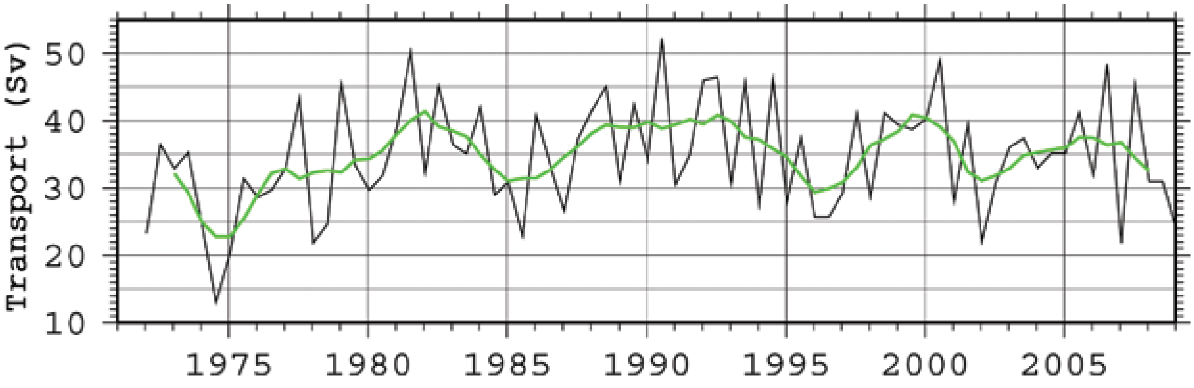

[Figure KU-8] Time series of the Kuroshio transport (Sv) along 137°E referenced to 1250 m depth. Thick green line indicates the 2 year running mean value.

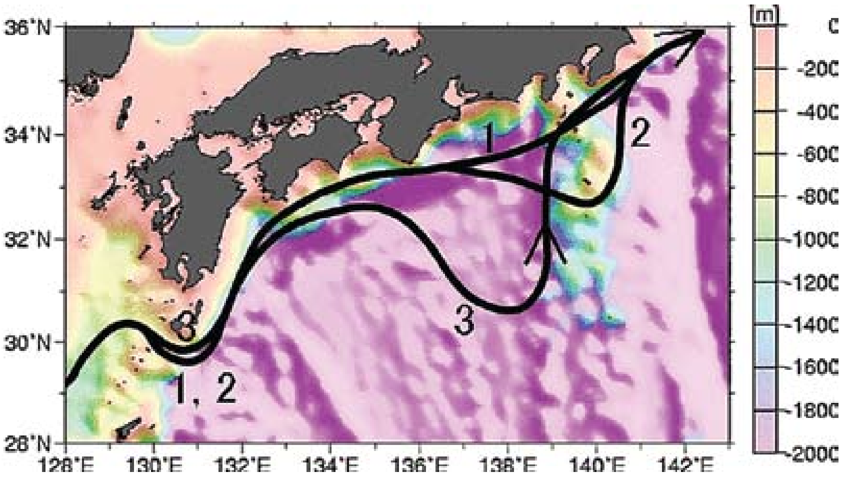

[Figure KU-9] Typical paths of the Kuroshio Current south of Japan: (1) nearshore Non-Large-Meander path (nNLM), (2) offshore Non-Large-Meander (oNLM), (3) typical Large-Meander (tLM).

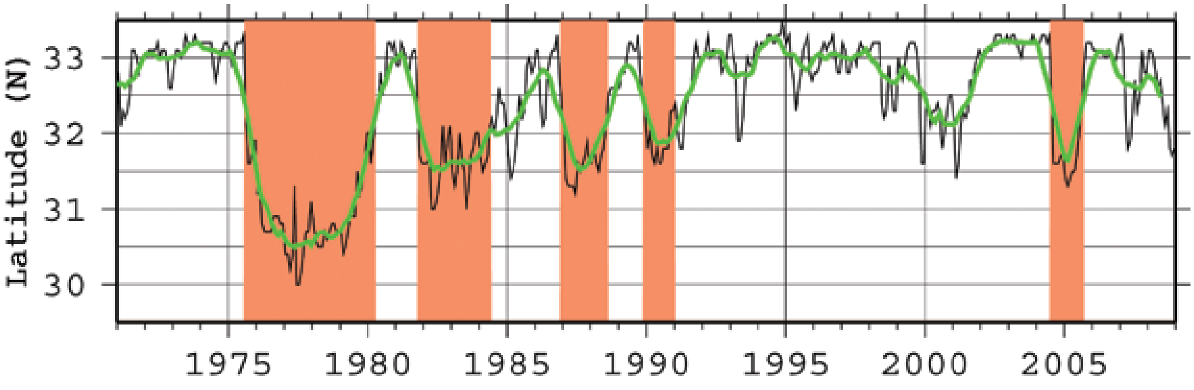

[Figure KU-10] The monthly southernmost latitude of the Kuroshio Current south of Japan (between 136°E and 140°E). The period when the Kuroshio took the Large Meander Path is shaded. The thick green line denotes the 13-month running mean value.

oNLM path in 2001). This implies that EOF2 and EOF3 are related to the meander pattern of the Kuroshio. It is likely that when the meander is east of 140°E, typical of the oNLM path, high temperature is observed in the coastal area west of 140°E because the warm Kuroshio passes near the coastal area, and low temperature is observed in the coastal area east of 140°E because the Kuroshio turns away from the coast. This meander pattern seems to affect EOF2. It is likely that when the meander is west of 135°E, the typical tLM path, low temperature is seen in the coastal area west of 140°E because the warm Kuroshio current runs away from the coast west of 140°E. This meander pattern seems to affect EOF3.

The volume of Kuroshio transport is thought to be related to atmospheric conditions. The relationship between wind conditions and Kuroshio transport in recent years has not been analyzed but unusually weak northwesterly wind was observed in 2007 (Fig. KU-3) and Kuroshio transport was low in 2007. The continued accumulation of both atmospheric and oceanic physical data is necessary to clarify the mechanisms determining transport and meandering of the Kuroshio.

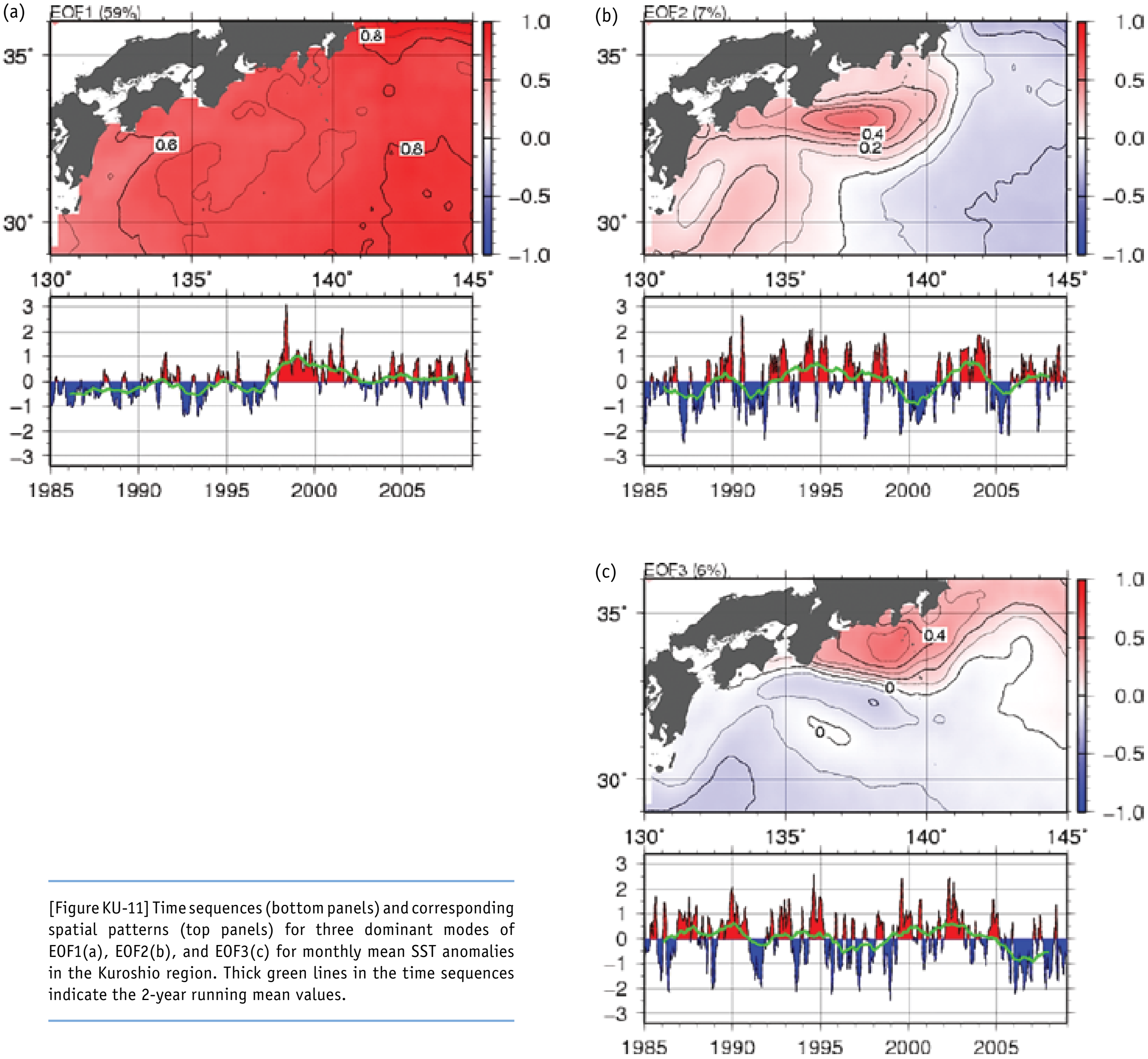

[Figure KU-11] Time sequences (bottom panels) and corresponding spatial patterns (top panels) for three dominant modes of EOF1(a), EOF2(b), and EOF3(c) for monthly mean SST anomalies in the Kuroshio region. Thick green lines in the time sequences indicate the 2-year running mean values.

3.2 Nutrients *(Sugisaki)*

Since 2001, the status of the Kuroshio ecosystem has been monitored along 138°E, called the O-line, by the Fisheries Research Agency of Japan (Fig. KU-13). Physical and biological data have been collected during seasonal research cruises in January, March, August and November using R/V *Soyo-maru*. Figure KU-12 shows the time series of nutrient concentrations at 15 depths from 0 m to 200 m at stations on the O-line from 2002 to 2008. Generally, nutrient concentrations are high during winter. The mixed layer is deep at this time because of seasonal wind and there is associated nutrient supply to the shallow layers from deeper layers. This supply of nutrients during winter supports high biological production in the Kuroshio ecosystem and most of the important pelagic fish species (e.g. Japanese sardine, Pacific saury etc.) spawn at this time. In recent years, especially since 2005, the seasonal pattern has become obscure and the average nutrient concentrations from 0 to 200 m have been significantly lower than in previous years. A decreasing trend in nutrient concentrations has also been observed in the Oyashio and Oyashio-Kuroshio transition areas and is attributed to shoaling of the mixed layer depth (Tadokoro et al. 2009) caused by an increase in temperature (Levitus et al. 2000). Positive anomalies of surface temperature in the Kuroshio region were observed from the late 1990s to the early 2000s (Fig. KU-11a), implying that a similar decreasing pattern in the long-term variation of nutrients has been occurring in western boundary current areas extensively throughout the North Pacific. In 2005, a significant meander of the Kuroshio was observed and the southernmost latitude of the Kuroshio was low compared to other years (Fig. KU-10). The meander causes a large gap between the Kuroshio and the high-nutrient coastal area. This may have restricted the supply of nutrients to Kuroshio water during 2005. Although the meander pattern of the Kuroshio returned from tLM to NLM (Fig. KU-10) after 2005, nutrient concentrations have remained low. There is no information or data explaining the mechanisms of this nutrient change but it is likely the same mechanism that causes the decreasing trend in the Oyashio; shoaling of mixed layer depth caused by climate change. Compared with the Oyashio, the pattern of change in nutrient concentration of the Kuroshio was stepwise and discontinuous. The change of the meander pattern of the Kuroshio may affect not only the supply of nutrients, but also may be a “trigger” of the manifestation of the distinct change of nutrients.

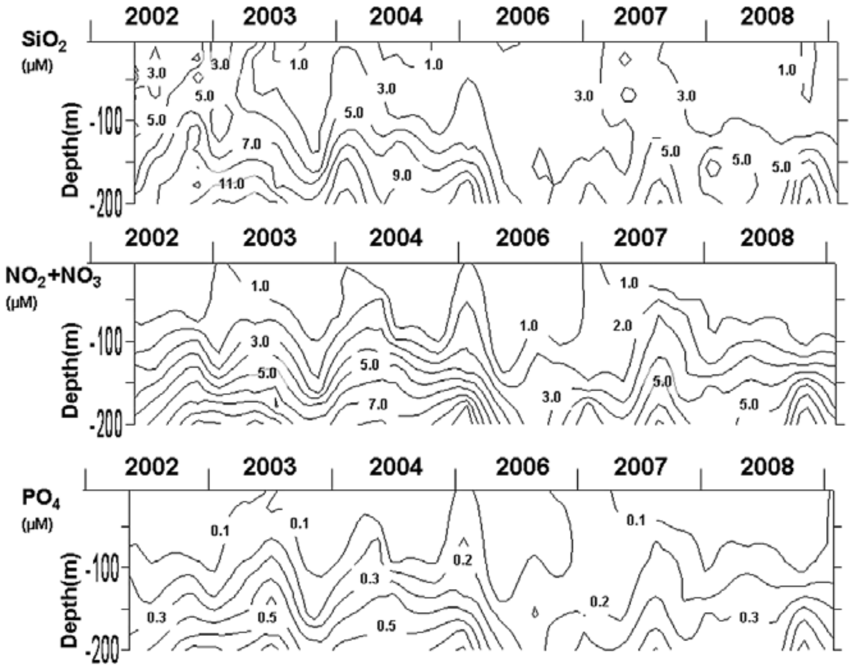

[Figure K-12] Time series of vertical nutrient concentrations (SiO2: upper, NO2 and NO3: middle, PO4: lower) between 0 and 200 m at a station on the Kuroshio axis of the O-line (138°E) during routine seasonal (January, May, August, November) cruises of each year.

3.3 Phytoplankton

3.3.1 Satellite chlorophyll *(Hidaka)*

Primary producers in the Kuroshio and slope water south of Honshu support important spawning grounds for pelagic fishes such as sardine, anchovy (*Engraulis japonicus*) and Pacific saury. The water south of the Kuroshio has different ecosystem properties and is influenced by fluctuations in the development of subtropical mode water. Satellite data provide an overview of geographical variation in surface ocean properties in the area (Fig. KU-13). Fig. KU-14 shows seasonal change of sea surface temperature (SST) and surface chlorophyll$_a$ concentration. The region can be divided into west (131°00'E-135°30'E) and east (135°30'E-139°00'E) sections at about Cape Shionomisaki and data compiled for the slope water and the Kuroshio in each section. Slope water is defined as the area between the 1000 m isobath on the continental slope and 56 km north of the Kuroshio axis. Slope water had higher chlorophyll$_a$ concentrations than the Kuroshio. The seasonal cycle of chlorophyll$_a$ in the Kuroshio was similar in the east and the west with a peak at the end of March. The pattern in the slope water in the western part was similar although chlorophyll$_a$ was higher than in the Kuroshio. The eastern part of the slope water showed a different seasonal pattern. Here, chlorophyll$_a$ started to increase from the end of February (day 24-40) and reached maximum values (0.71-0.85 µg·l^{-1}) in March (day 72-104) as in the western part. But the chlorophyll$_a$ pattern after mid-March differed and high chlorophyll$_a$ (>0.6 µg·l^{-1}) remained until mid-May (ca. day 132).

Seasonal variation of chlorophyll$_a$ is well synchronized with SST in both regions. Blooms start at the end of the low temperature season (day 60-90) and decrease as SST increases (day 120-240). The trends described above were consistent between the focal period and a previous

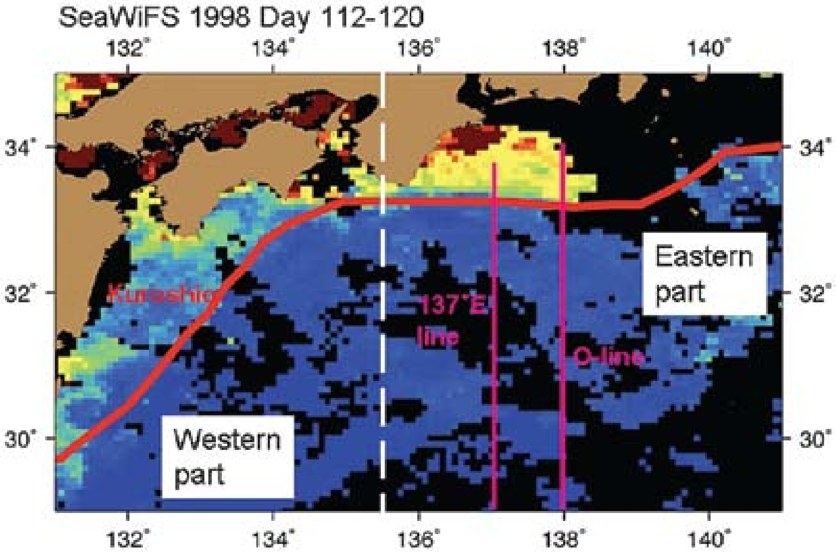

[Figure KU-13] The area analyzed for phytoplankton in the Kuroshio region.

period (1998-2002) in each area. Because the nutrient concentrations changed after 2005 (large meander year), seasonal variations of chlorophyll$_a$ and SST were compared before (2003-2004) and after (2005-2007) the large meander. Except for the eastern part of the Kuroshio, higher peaks of chlorophyll$_a$ were observed during late winter and early spring (day 60-120) in 2003-2004 than in 2005-2007. On the other hand, chlorophyll$_a$ values in 2005-2007 were similar or higher than 2003-2004 after day 180. This shows that the characteristic seasonal variation of chlorophyll$_a$ (high in spring and low after summer) became obscure after 2005. Because SST patterns were not clearly different between 1998-2002 and 2003-2007, no relationships between SST and chlorophyll$_a$ were seen at this time. Although mechanisms causing the difference in the seasonal pattern of chlorophyll$_a$ between 2003-2004 and 2005-2007 are not known well, the large meander that occurred from late 2004 to early 2005 may have affected the distribution of nutrients which subsequently caused the changing seasonal patterns.

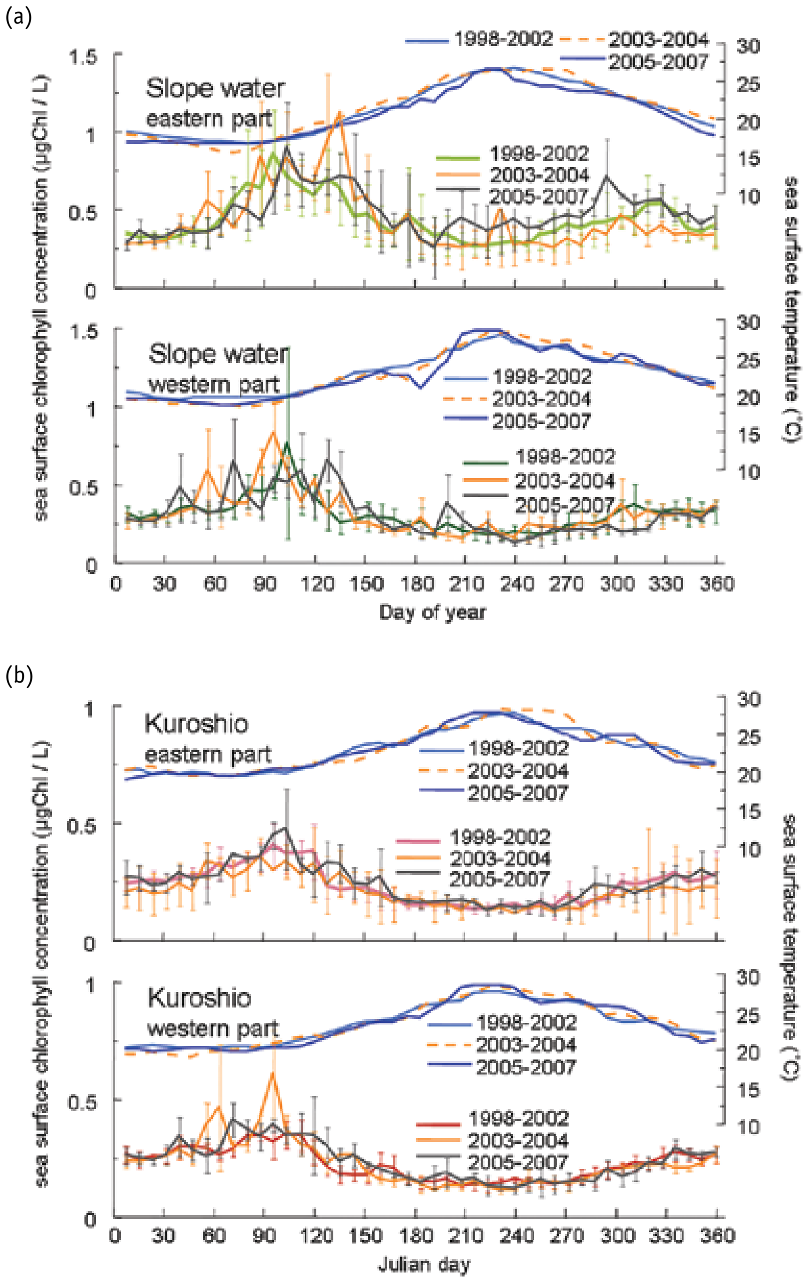

[Figure KU-14] Seasonal change of sea surface chlorophyll$_a$ concentration and sea surface temperature in the slope water (a) and Kuroshio (b). Sea surface temperature (SST) was derived from the 8-day averaged AVHRR dataset (pathfinder ver. 5.0, 8-days, 1990-2002, distributed by the NOAA-National Oceanographic Data Center). The line graph of SST was developed using a moving average representing 3 sets of 8-day data to smooth variability. Error bar means SD.

3.3.2 Species composition *(Sugisaki, Hidaka)*

Long-term monitoring of phytoplankton species composition in the Kuroshio region is limited. The Japan Meteorological Agency occupies a meridional line for field observation along 137°E and the Fisheries Research Agency has another line along 138°E (the O-line) but coverage of each line is limited. The 137°E line is investigated once or twice per year and observations on the O-line began only in 2002. On the O-line program, taxonomic composition of phytoplankton has been monitored at two stations, one in the slope water (34°N 138°E) and another in the offshore water south of the Kuroshio (30°N 138°E). Fig. KU-15 shows the composition of diatom genera at 34°N late in the spring phytoplankton bloom (May). The dominant genera are variable among years but *Rhizosolenia* (most dominant in 2003, 2006, 2007) and *Cylindrotheca* (>20% in 2004 and 2005) were important. The diatom composition is influenced by the phenology of the phytoplankton bloom and the nutrient conditions, the latter being influenced by both vertical mixing and horizontal advection. Controls on the annual variation of phytoplankton species composition are not clear but high biomass and change of species composition were observed in 2004. The Kuroshio meander was also observed during 2004 and 2005 (Fig. KU-10). It is possible that Kuroshio oceanic water intruded into the near-shore area of the Kuroshio region because of the Kuroshio Countercurrent, causing the oceanic genera *Chaetoceros* and *Cylindrotheca* to become abundant in these years.

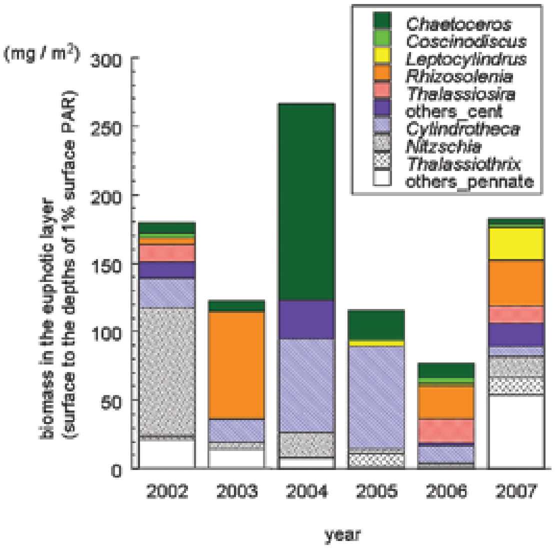

[Figure KU-15] Composition of diatoms in the euphotic zone at Station B03 (34°N 138°E) in May.

3.3.3 Timing of the spring bloom *(Kameda)*

Since it is likely that the timing of the spring bloom is sensitive to climate change, its annual variation was analyzed using objective indices that were originally developed to characterize the spring phytoplankton bloom on the Nova Scotia-Labrador shelf (Fuentes-Yaco et al. 2007). Bloom initiation, date of the maximum, and bloom duration were determined for slope water and the Kuroshio from satellite data. SeaWiFS data cover the period from 1998 to 2007 (Fig. KU-16). Indices were averaged by year and area. Though distinct trends in timing of the spring bloom were not observed, interannual differences in bloom timing and duration were evident. In the western part of the slope water, the spring bloom began earlier in 2006 and 2007 than in other years (1998 to 2005). In the eastern part of the slope water, bloom initiation was early in 2002 and 2003 and showed a progressive delay in the period from 2004 to 2007. In the Kuroshio area, the spring bloom started earlier in the western part than in the eastern part before 2004 but this pattern was not seen after 2005.

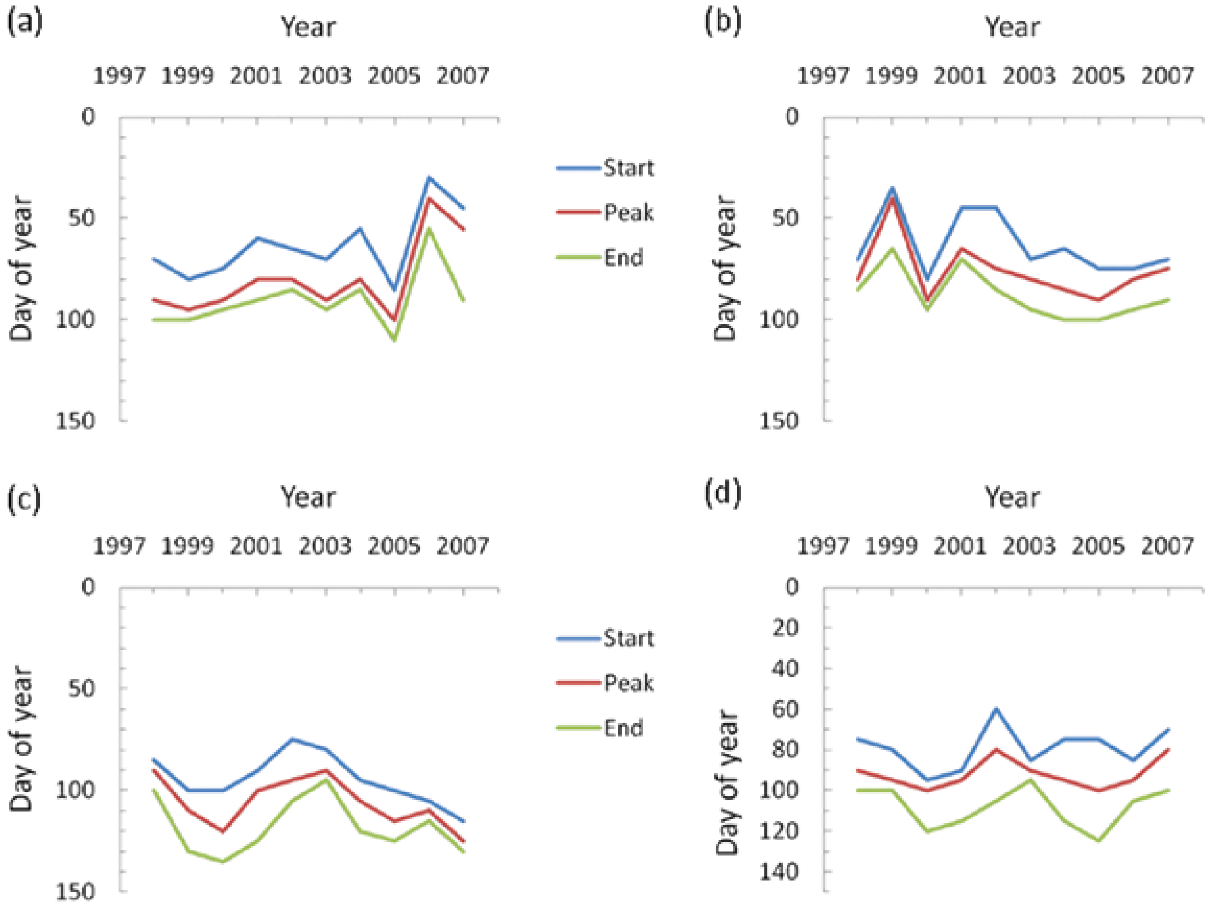

[Figure KU-16] Phytoplankton spring bloom characteristics: (a) Slope water western part (b) Kuroshio western part (c) Slope water eastern part (d) Kuroshio eastern part.

© Hyung-Ku Kang

4.0 Zooplankton *(Hirota, Sugisaki)*

Interannual changes of zooplankton in the Kuroshio and surrounding area before 2002 have been reported (e.g. Shimizu et al. 2004; Nakata and Hidaka 2003) but there have been few observations since 2003. Hydrographic conditions in the Kuroshio and the surrounding area allow three areas to be distinguished, the onshore side of the Kuroshio, the main stream zone of the Kuroshio and the offshore side of the Kuroshio. Since the character of the Kuroshio varies according to location, the mainstream zone of the Kuroshio on the west side of Cape Shionomisaki south of Japan was defined by temperatures higher than 16.5°C at 200 m depth and with flow >1 $m \cdot s^{-1}$ at the surface, and the zone on the east side of Cape Shionomisaki was defined by temperatures higher than 15°C at 200 m depth (Kawai 1969) in this section.

The 18 year mean zooplankton biomass from 1971 to 1988 in the western area (south of Kyushu to south of Cape Shionomisaki) of the Kuroshio during January and February was 439.45 $\mu gC \cdot m^{-3}$, and positive anomalies of 0-400 $\mu gC \cdot m^{-3}$ were observed in the first half of the 1970s. After 1976, the anomaly fluctuated between -400 and +50 $\mu gC \cdot m^{-3}$ until 1988. The 19 year mean zooplankton biomass from 1971 to 1989 in the eastern area of Kuroshio (from south of Cape Shionomisaki to south of the Enshu-nada region, called "central Japan" in the original paper of Nakata and Koyama 2003) during February and March was 854.49 $\mu gC \cdot m^{-3}$, and positive anomalies of 0-400 $\mu gC \cdot m^{-3}$ were observed in the first half of the 1970s. After 1976, the anomaly fluctuated between -300 to +50 $\mu gC \cdot m^{-3}$ until 1989 (Nakata and Koyama 2003). The zooplankton biomass anomaly in winter (January and February) of 1972-2000 on the line of 137°E became negative in the

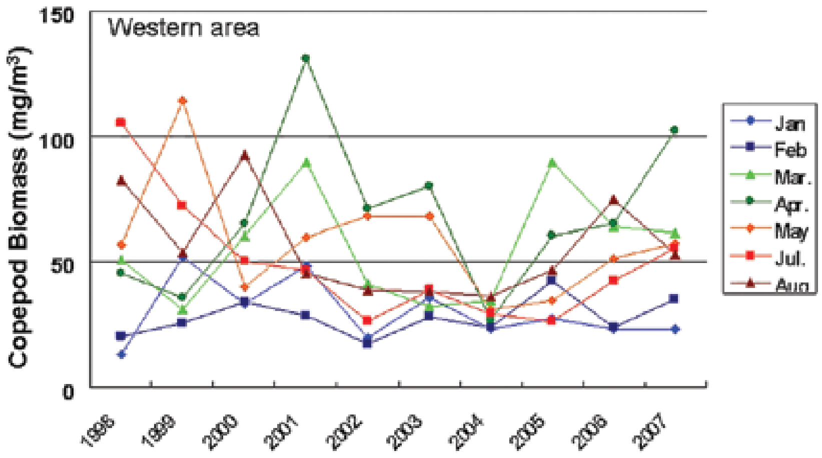

[Figure KU-17] Zooplankton biomass (wet weight $mg \cdot m^{-3}$) from samples collected in the day time with a NORPAC net of 0.33-0.35 mm mesh aperture towed vertically from 200 m to surface in January to February of 1998-2007 in the western area of the onshore side of the Kuroshio.

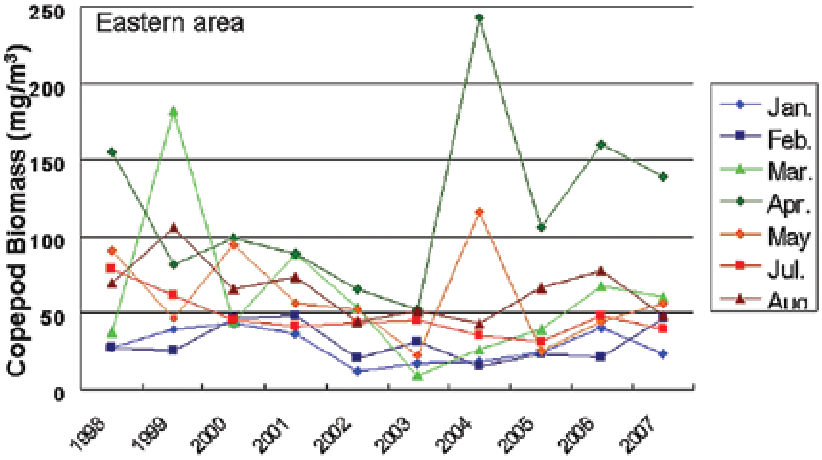

[Figure KU-18] Zooplankton biomass (wet weight $mg \cdot m^{-3}$) from samples collected in the day time with a Norpac net of 0.33-0.35 mm mesh aperture towed vertically from 200 m to surface in March to May of 1998-2007 in the eastern area of the onshore side of the Kuroshio.

first half of the 1970s and positive in the latter half of the 1970s and then it continued negative until 1994 (Nagai 2004). The zooplankton biomass anomaly during July and August was positive in the first half of the 1970s and generally became negative from 1976 to 1994 (Nagai 2004). In sum, a decreasing trend in zooplankton biomass was observed in the Kuroshio region before 2000.

Research on the oceanography, zooplankton biomass and distribution of larval fish and eggs has been conducted by the National Research Institute of Fisheries Science, Fisheries Research Agency for many years. Data collected at the stations in the western area between 31° and 34°N and 131° and 136°E with associated water temperature at 200 m depth <16.5°C and the stations in the eastern area between 32° and 36°N and 136° and 140°E with associated water temperature at 200m depth <15°C were analyzed in order to observe the annual and seasonal variations of zooplankton biomass. In both areas, the daytime zooplankton biomass in summer (July and August) generally decreased from 1998 to 2005 and increased after 2005 (Figs. KU-17, 18). Winter biomass (January and February) was low and did not vary annually. The spring biomass (March, April and May) was highly variable among years and month of maximum biomass has gradually changed from May to March in the western area.

Figure KU-19 shows interannual and seasonal variation in biomass (volume) of copepods at a fixed single station (33°12'N, 133°46'E). Although high abundance was observed during March and April in the 1990s, only weak seasonality has been observed since the early 2000s. The dominant species in this area, *Calanus sinicus*, also showed an increase during March and April, though only a small peak has been observed during July since the late 1990s (Fig. KU-20). Thus, the seasonal variation of copepod biomass has become weak to non-existent and the seasonal pattern of the dominant copepod species has changed in recent years.

The biomass of chaetognaths and crustaceans other than copepods was correlated with wind speed at Cape Shionomisaki (Nakata and Koyama 2003). The biomass of large copepods (prosome length ≥1 mm) in the mainstream zone of the central area in the winter (February to March) of 1971-2000 was positively correlated to the Southern Oscillation index, while the biomass of small copepods (prosome length <1 mm) changed in cycles of 2-4 years. These changes are related to regional climate factors like the meander of the Kuroshio, surface temperature, and the average temperature between 0 and 200 m (Nakata and Hidaka 2003). The interannual changes of zooplankton biomass in the offshore side of the Kuroshio (30-32°N) on the 137°E line in winter was negatively correlated with the wind speed between 25-35°N and the depth of the mixed layer between 30-32°N (Sugimoto and Tadokoro 1998). The zooplankton biomass south of Shikoku and south of the Kii peninsula (28-32°N, 132-137°E) in January to March of 1971-2001 was positively correlated with the depth of the winter mixed layer (Limsakul et al. 2001; Chiba et al. 2008). Zooplankton biomass in the spring (April to June) of 1974-2002 in the same area (28-32°N, 132-137°E) was positively correlated with the depth of the winter mixed layer in the offshore side of the Kuroshio (Chiba et al. 2008). The interannual change in wet weight of zooplankton at stations on the line of 137°E in the Kuroshio mainstream and Kuroshio Countercurrent during 1972-2000 was positively correlated with chlorophyll$_a$ (Nagai 2004). In and offshore of the Kuroshio, the winter mixed layer becomes deeper during strengthening of the Aleutian Low, more nutrients were supplied to the mixed layer, and the biomass of phytoplankton and zooplankton increased in spring.

Average zooplankton biomass at PN1 in the Kuroshio Countercurrent (27.5°N, 128°E) from 1973-2002 tended to decrease. Moreover, the interannual changes of zooplankton biomass, the number of chaetognaths, *Pterosagitta draco*, and the concentration of phosphate varied similarly to the MOI (monsoon index) (Shimizu et al. 2004).

After 2000, a clear trend in zooplankton biomass was not observed even though there was a decreasing trend in nutrients and phytoplankton. In contrast to previous studies, relationships between zooplankton biomass and climate indices were not obvious. On the other hand, geographical differences in zooplankton biomass were observed. For example, extremely high biomass of zooplankton during spring (March or April) was observed frequently in the eastern area but not in the western area. These differences imply that Kuroshio water transports and accumulates nutrients or organic matter as it flows along the southern Japanese archipelago. The transportation and accumulation status may vary according to the status

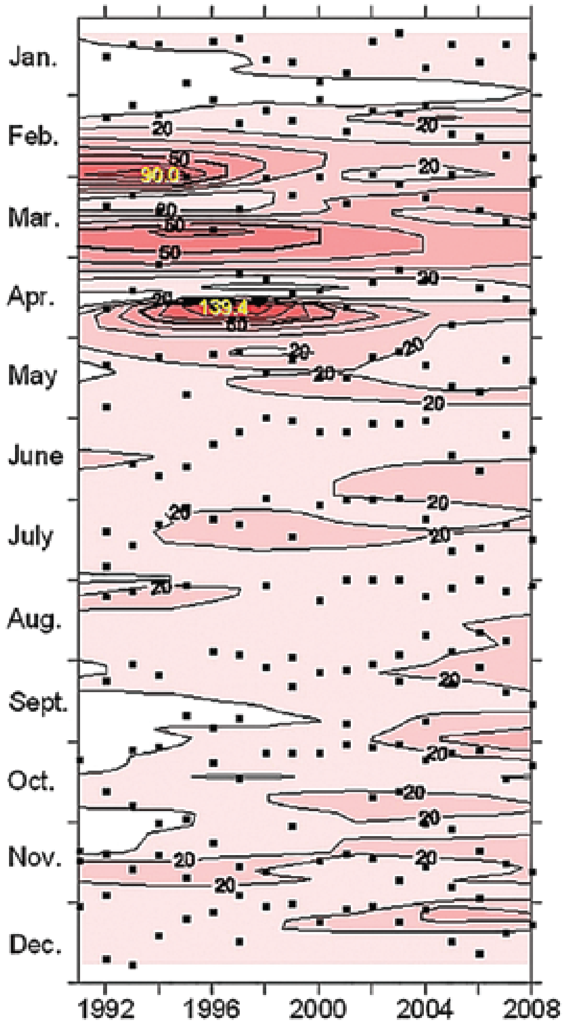

[Figure KU-19] The seasonal and annual variations of volume ($mm^3 \cdot m^{-3}$) of copepods collected with a NORPAC net towed vertically from 200 m to the surface at a single station (33°12′N, 133°46′E) in 1991 to 2008.

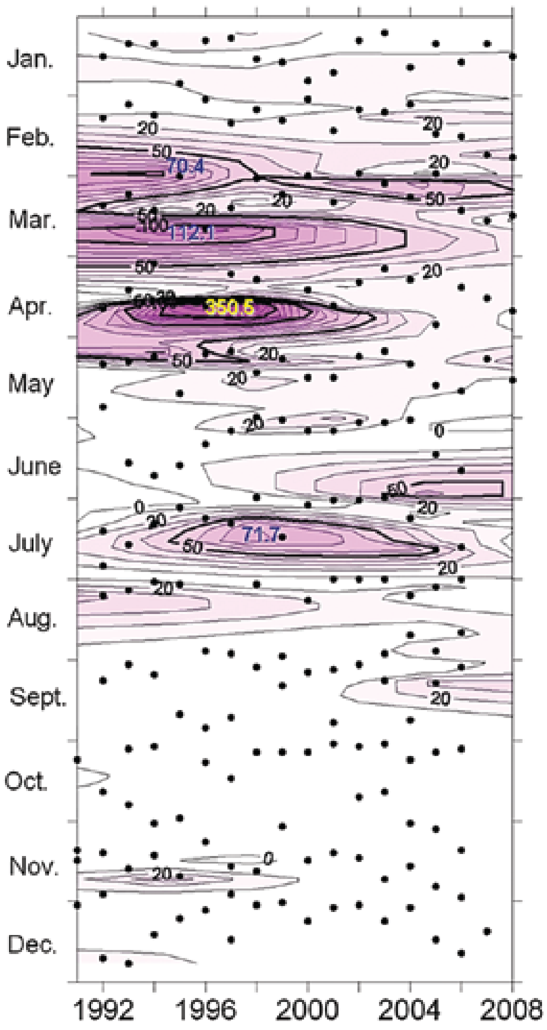

[Figure KU-20] The seasonal and annual variations of the abundance (inds.$\cdot m^{-3}$) of *Calanus sinicus* collected with a NORPAC net of 0.33 mm in mesh aperture towed vertically from 200 m depth to the surface at a single station (33°12′N, 133°46′E) in 1991 to 2008.

of the Kuroshio meander. For example, a clear meander of the Kuroshio was observed in 2004 and 2005 and a reduction of zooplankton biomass was observed especially during the high biomass season (March and April) in 2004 in the western area (Fig. KU-17). On the other hand, high biomass in April and May were observed in 2004 in the eastern area, and the importance of April has been sustained since 2004 (Fig. KU-18). Large peaks in zooplankton volume (>60 $mm^3 \cdot m^{-3}$) were observed during spring (February to April) before 2004, while the spring peaks were low (<40 $mm^3 \cdot m^{-3}$) after 2004. Late in the year (August to December) relatively high volumes (>20 mm3$\cdot m^{-3}$) were observed since 2004 although the volume was usually <20 $mm^3 \cdot m^{-3}$ before 2004 (Fig. KU-19). This implies that seasonal variation of zooplankton biomass has become obscure in recent years. It seems that the seasonal variability of zooplankton has been changing since 1998. Mechanisms causing variation of zooplankton biomass are not fully understood but data to date imply that physical conditions, not only wind or temperature but also the meander of the Kuroshio, are important in this region.

5.0 Fishes and Invertebrates

(Oozeki, Takasuka, Kubota)

The Kuroshio system plays an important role in reproduction, dispersal, and migration of pelagic fish species including squid. Small pelagic fish species which are distributed off the Pacific coast of Japan include the Japanese sardine, Japanese anchovy, chub mackerel (*Scomber japonicus*), spotted mackerel (*Scomber australasicus*), round herring (*Etrumeus teres*), jack mackerel (*Trachurus japonicus*), Pacific saury and Japanese common squid (*Todarodes pacificus*). They utilize the Kuroshio system as a spawning ground and as the mechanism for dispersing the larval and juvenile stages from southern to northern areas of the western North Pacific. These animals migrate northward through the Kuroshio-Oyashio transition region to the Oyashio region where they are caught in fisheries. In the Kuroshio system, skipjack tuna (*Katsuwonus pelamis*), blue shark (*Prionace glauca*) and neon flying squid (*Ommastrephes bartrami*) are important predators on small pelagic fishes. Top predators such as whales and seals also feed on these small pelagic fishes in the Kuroshio Extension region.

Spatial and temporal variability of spawning habitat are composites of environmental forcing factors, spawning stock biomass, and vital parameters of spawning fish (e.g. temperature preference and food requirement). Reproductive and survival strategies are expected to be tightly linked to habitat use, extent of spawning, and responses to environments. Such biological characteristics can differ even among co-occurring congeners. For example, temperature and salinity diagrams discriminated spawning habitats of small pelagic fishes in the Kuroshio system (Oozeki et al. 2007a). As well, recent studies from the other regions showed that biological factors such as chlorophyll$_a$ concentration also serve as determinants of spawning habitat (Reiss et al. 2008). Small pelagic fishes tend to exhibit offshore expansion and inshore contraction in spawning habitat and distribution area depending on their stock size, but the habitat occupation strategy could differ between the anchovy and sardine (Barange et al. 2009). Judging from the information on spawning grounds and distributions, recent physical and biological conditions seem to favor the species which are known to be abundant during warm-sea-surface periods (Japanese anchovy, Japanese common squid, and Pacific saury) and do not seem to favor the species which are known to be abundant during cool-sea-surface periods (Japanese sardine). Further studies of species-specific responses to environmental factors and the decadal-scale shifts in spawning habitats associated with physical and biological environments would promote understanding of mechanisms linking environmental conditions to spawning ground formation, and allow discussion of recent trends in the context of ecosystem changes. The general dynamics and recent status of the spawning grounds are described below for the major small pelagic fish species in the Kuroshio system.

5.1 Japanese sardine

(Sardinops melanostictus)

The Japanese sardine is distributed off the Pacific coast of Japan (the Pacific stock) and its range fluctuates depending on stock size (Checkley et al. 2009). Biomass has been very low during the last decade (Anonymous 2009; Checkley et al. 2009). Accordingly, distribution and spawning areas have shrunk and egg abundance has been at a low level during recent years. In general, the eastern boundary of sardine distribution has been considered to be ca. 155°E longitude during low-biomass periods. However, recent studies revealed that the northern limit of migration was offshore of north Kuril Island (46°N 165°E) and that the eastern boundary was extended beyond 180° even during the low-biomass period (Kawabata et al. 2008a; Anonymous 2009). The southern and western boundaries were 29°N and 129°30'E, respectively. The southern boundary of distribution coincided with that of the spawning grounds. Spawning grounds of the Pacific stock were located in the coastal areas from 31°N 131°E to 41°N 142°E and mainly around Tosa Bay from 32°N 132°E to 33°N 135°E during the low-biomass periods of 1997-2004 (Fig. KU-21) (Mori et al. 1988; Kikuchi and Konishi 1990; Ishida and Kikuchi 1992; Zenitani et al. 1995; Kubota et al. 1999; Oozeki et al. 2007a). The sum of the total annual egg production of the Pacific stock over all the areas off the Pacific coast of Japan was low, from 38×10^{12} to 152×10^{12} eggs, during the period from 2005 to 2007 and the main spawning ground was located in a limited area around Tosa Bay during that period. Spawning occurs from October to May and juveniles are transported by and migrate to the Kuroshio and Kuroshio Extension currents beyond 170°E in spring. Feeding grounds are typically located in the Oyashio and Kuroshio-Oyashio

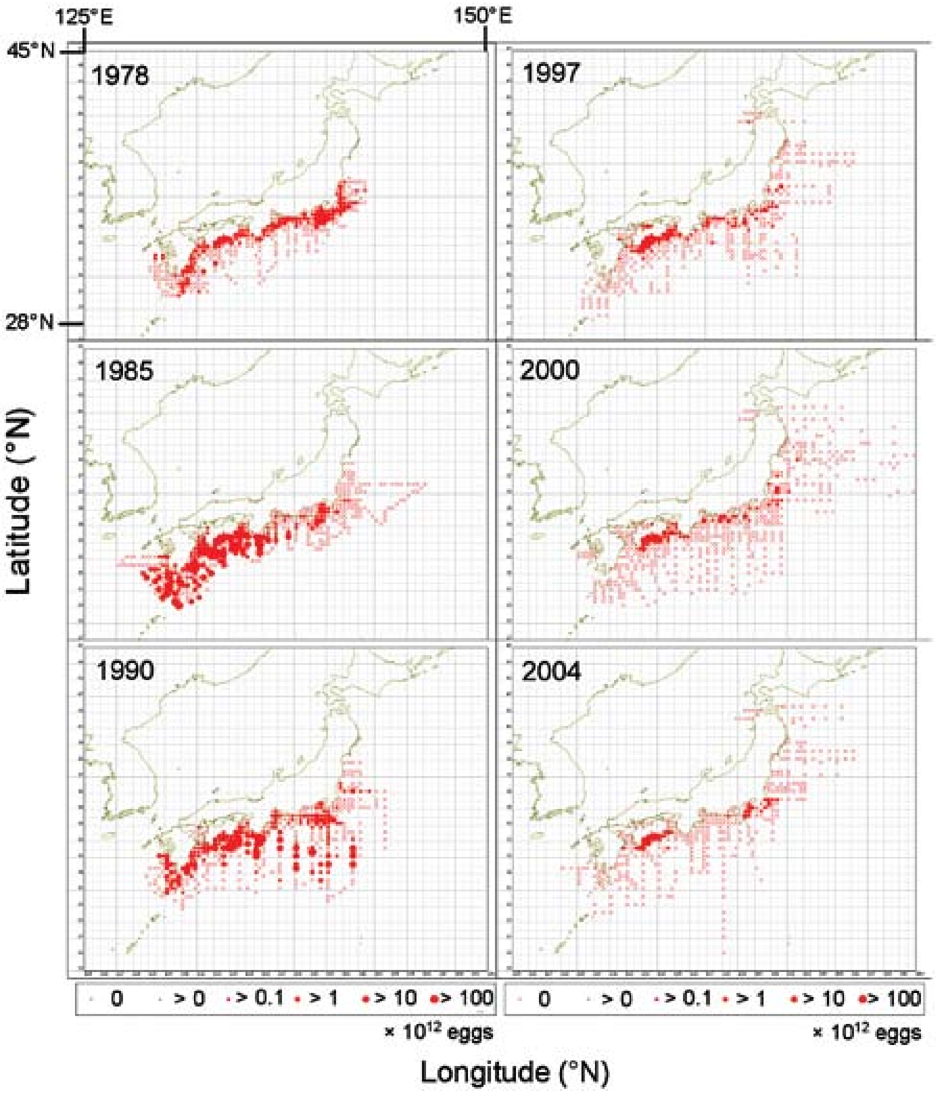

[Figure KU-21] Total egg production (eggs per year per 15′×15′ square) of Japanese sardine *Sardinops melanostictus* from 1978 to 2004. The data were collected from fish egg and larval fish research coordinated by the Fisheries Agency of Japan (Anon. 2006-2008; Anon. 2009).

Transition regions, from 42°N 144°E to 45°N 55°E, in summer and autumn. Adult fish migrate southward to their spawning grounds in late autumn and winter. Young of the year fish tend to be retained in the middle of their spawning migration path offshore of the Joban area (35-37°N 141-143°E).

5.2 Japanese anchovy *(Engraulis japonicus)*

The Japanese anchovy is distributed off the Pacific coast of Japan with an eastern boundary of ca. 155°E during low-biomass periods and beyond 180°E during high-biomass periods (Anonymous 2009). The Pacific stock of anchovy has been at a high-biomass level during the past decade, and thus the distribution and spawning areas are currently expansive. The southwestern boundary was observed around 29°N 129°E and the northern limit of its migration area corresponded to the offshore area of north Kuril Island, 46°N 165°E (Kawabata et al. 2008a). Spawning grounds of the Pacific stock were located in coastal areas from 32°N 131°E to 38°N 142°E during the low-biomass periods in 1978 and 1985 (Fig. KU-22) (Mori et al. 1988; Kikuchi and Konishi 1990; Ishida and Kikuchi 1992; Zenitani et al. 1995; Kubota et al. 1999; Oozeki et al. 2007a). During the high-biomass periods,

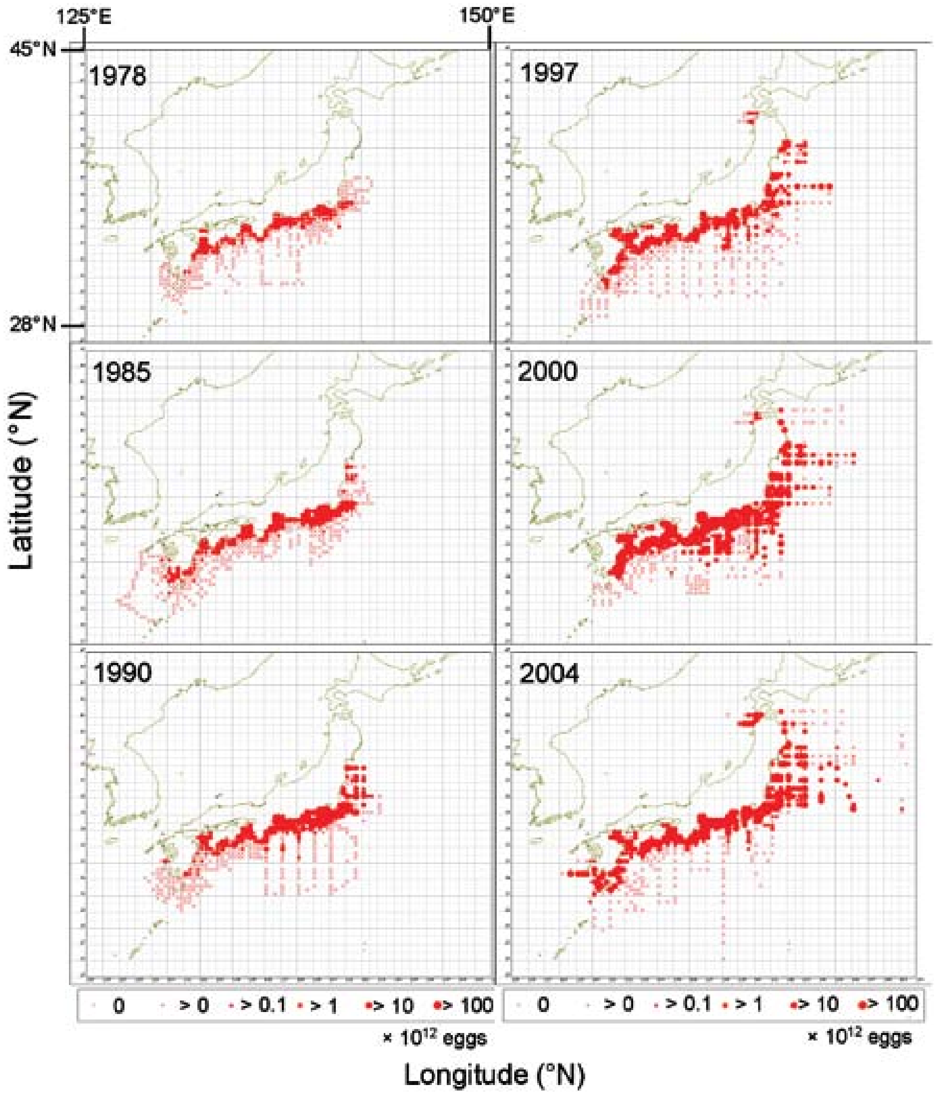

[Figure KU-22] Total egg production (eggs per year per 15′×15′ square) of Japanese anchovy (*Engraulis japonicus*) from 1978 to 2004. The data were collected from fish egg and larval fish research coordinated by the Fisheries Agency of Japan (Anon. 2006-2008; Anon. 2009).

spawning was observed not only in the inshore areas off the Pacific coast but also in the offshore areas beyond the Kuroshio axis, from 29°N 130°E to 43°N 155°E and also in the Kuroshio-Oyashio transition region (1990-2004 see Fig. KU-22). Active spawning in the coastal area of the Kuroshio-Oyashio transition region has continued from 2005 to 2008 and total annual egg production ranged from $10,000\times10^{12}$ to $12,100\times10^{12}$ eggs during 2005 to 2007. Spawning occurs from February to October and juveniles are transported by the Kuroshio and Kuroshio Extension currents beyond 170°E longitude in spring. Feeding grounds are typically located in the Oyashio and Kuroshio-Oyashio transition regions, from 42°N 144°E to 45°N 155°E, in summer and autumn. Adult fish migrate southward to the spawning grounds in late autumn. Young of the year fish tend to be retained in the middle of their spawning migration path (35-37°N 141-143°E).

5.3 Chub mackerel *(Scomber japonicus)*

The chub mackerel is widely distributed from the waters off Kyushu Island to the Pacific coast of northeastern Japan. Chub mackerel migrate seasonally along the Pacific coast of Japan from Kyushu to Hokkaido and feed on larvae and juveniles of small pelagic fishes during their migration.

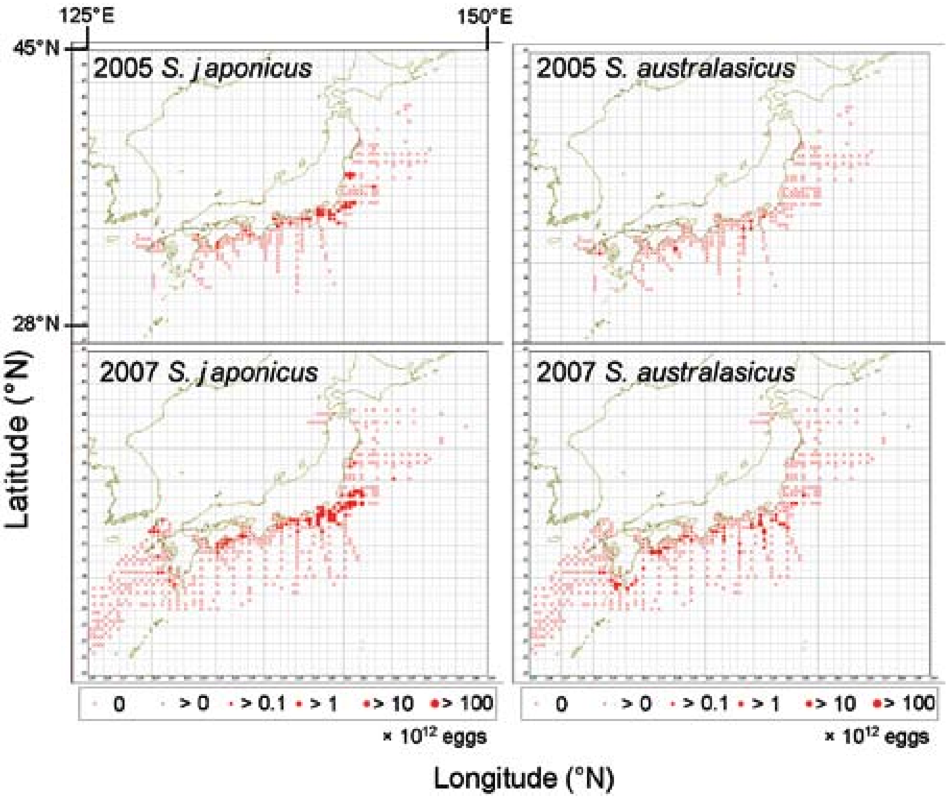

[Figure KU-23] Total egg production (eggs per year per 15′×15′ square) of chub mackerel (*Scomber japonicus*) and spotted mackerel (*Scomber australasicus*) in 2005 and 2007. The data were collected from fish egg and larval fish research coordinated by the Fisheries Agency of Japan (Anon. 2006-2008; Anon. 2009).

Spawning occurs from March to July in the waters mainly around the Izu Islands, near central Japan (Fig. KU-23) (Watanabe 1970; Usami 1973; Murayama et al. 1995; Watanabe et al. 1999; Anonymous 2006-2008). Total annual egg production ranged from 38×10^{12} to 280×10^{12} eggs during 2005 to 2007. After spawning, adults and their offspring migrate northeast and are distributed throughout the feeding ground in the Kuroshio-Oyashio transition area and in the Oyashio (Odate 1961; Kawasaki 1966; Watanabe 1970; Watanabe and Nishida 2002). In autumn, juveniles and adults migrate south to the Joban area. Juveniles usually overwinter in the coastal waters off Joban, and mature fish migrate farther south to the spawning grounds around the Izu Islands (Watanabe 1970; Usami 1973).

5.4 Spotted mackerel *(Scomber australasicus)*

The spotted mackerel is distributed in relatively warm waters compared to chub mackerel. Although spotted mackerel were confined to the Kuroshio system as their northern limit until the 1980s, their distribution areas have expanded up to 43°N along the Pacific coast of Hokkaido in recent years (Anonymous 2009; Kawabata et al. 2008b). The one-year old fish are mainly distributed in the Oyashio and Kuroshio-Oyashio Transition regions from 37°N to 45°N and 142°E to 170°E in summer and autumn. Recent developments in the taxonomy of mackerel eggs (Meguro 2008) have allowed the spawning grounds of chub mackerel and spotted mackerel to be separated. The spawning ground of chub mackerel has a range from 30°N to 37°N during recent years, although their major spawning ground is thought to be located in the East China Sea (Fig. KU-23). The main spawning ground has shifted from the southern area of Japan to the coastal area of the Boso peninsula and around the Izu Islands. Total annual egg production ranged from 4×10^{12} to 64×10^{12} eggs during 2005 to 2007.

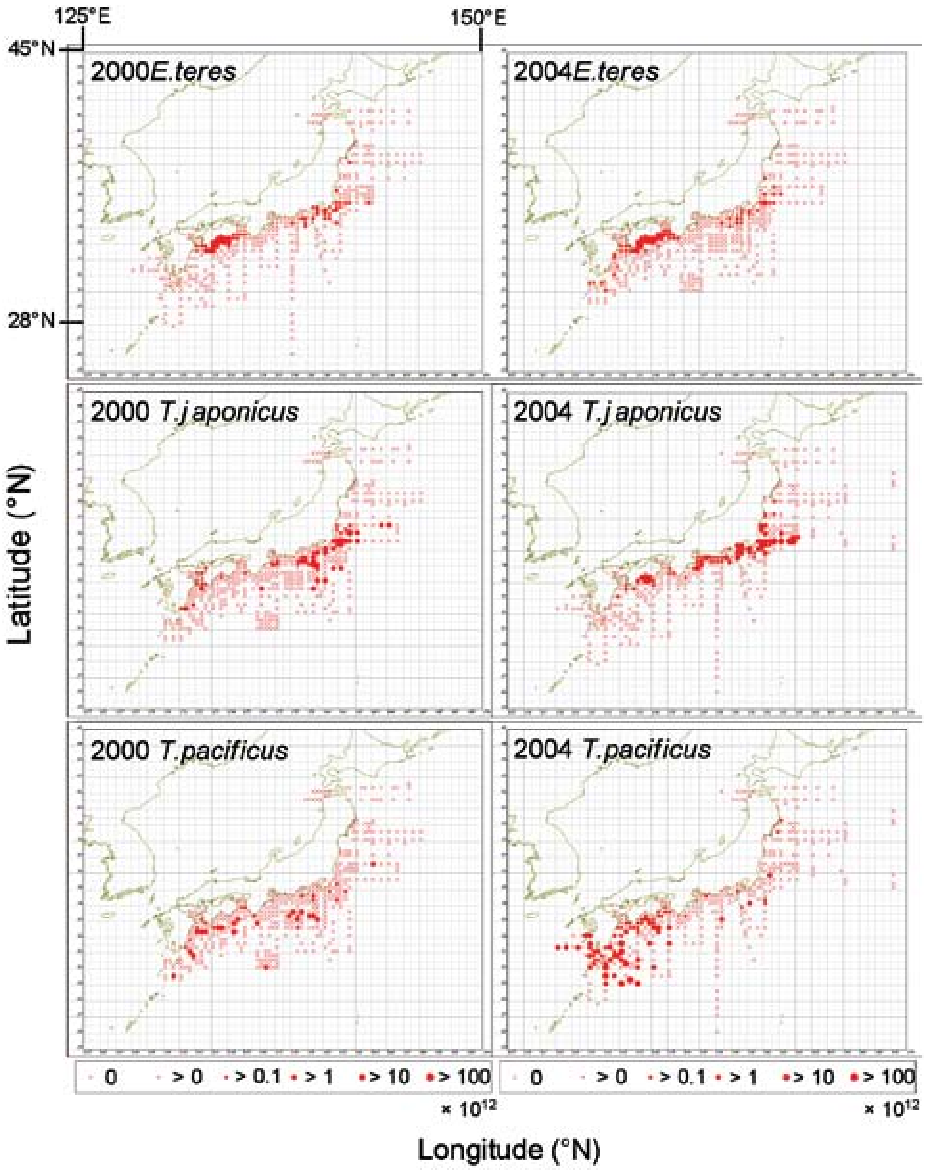

[Figure KU-24] Total egg production (eggs per year per 15′×15′ square) of round herring (*Etrumeus teres*), and larval densities of jack mackerel (*Trachurus japonicus*) (yolk-sac larvae) and Japanese common squid (*Todarodes pacificus*) (rhynchoteuthion paralarva) in 2000 and 2004. The data were collected from fish egg and larval fish research coordinated by the Fisheries Agency of Japan (Anon. 2006-2008).

5.5 Round herring *(Etrumeus teres)*

Round herring are distributed mainly along the southern Pacific coast of Japan with their northern boundary at 38°30'N. The population size of Pacific round herring is stable compared to Japanese sardine and anchovy (Anonymous 2009). The distribution areas of the Pacific stock roughly correspond to the spawning grounds, and the southwestern boundary of their habitat was observed around 29°N 129°30'E, which coincided with the southern boundary of the spawning ground (Fig. KU-24). The main spawning grounds were in the coastal areas of Tosa Bay from 32°30'N 132°30'E to 33°30'N 135°E (Mori et al. 1988; Kikuchi and Konishi 1990; Ishida and Kikuchi 1992; Zenitani et al. 1995; Kubota et al. 1999). Total annual egg production ranged narrowly from 130×10^{12} to 177×10^{12} eggs during 2005 to 2007.

5.6 Japanese common squid *(Todarodes pacificus)*

Common squid around Japan are distinguished as either a winter spawning population or an autumn spawning population, although some spawning activities are observed all year round. The abundance of common squid has been relatively high during the last decade and their spawning grounds are currently broadly distributed. The spawning ground of the winter population is thought to be located in the East China Sea as rhynchoteuthion paralarvae are widely observed from February to May along the Kuroshio Current (Fig. KU-24) (Anonymous 2009). The paralarvae are transported to northern areas by the Kuroshio and juveniles are widely observed in the Kuroshio-Oyashio transition region. The distribution of immature adults extends to the southern coast of Hokkaido Island on the Pacific side. Mature adults can migrate westward via Soya Strait or Tsugaru Strait toward their spawning grounds.

5.7 Pacific saury *(Cololabis saira)*

Pacific saury is a widely distributed pelagic species in the northwestern Pacific. Spawning extends from autumn to late spring from the Kuroshio to the Kuroshio-Oyashio transition regions. Survival after hatching controls recruitment in autumn and spring in the transitional waters. High growth rates lead to low mortality in the Kuroshio waters in the winter spawning season (Watanabe et al. 2003). The spawning ground of Pacific saury has expanded offshore from the Kuroshio Axis to 32°N 160°E as their southern and eastern limit (Fig. KU-25) (Oozeki et al. 2007b) and the juveniles of Pacific saury utilize the clockwise current in the Kuroshio recirculation region to come back to the Kuroshio system, and then migrate northward to reach their feeding ground from the coast of Hokkaido to the offshore area of north Kuril Island (46°N 165°E) from spring to summer.

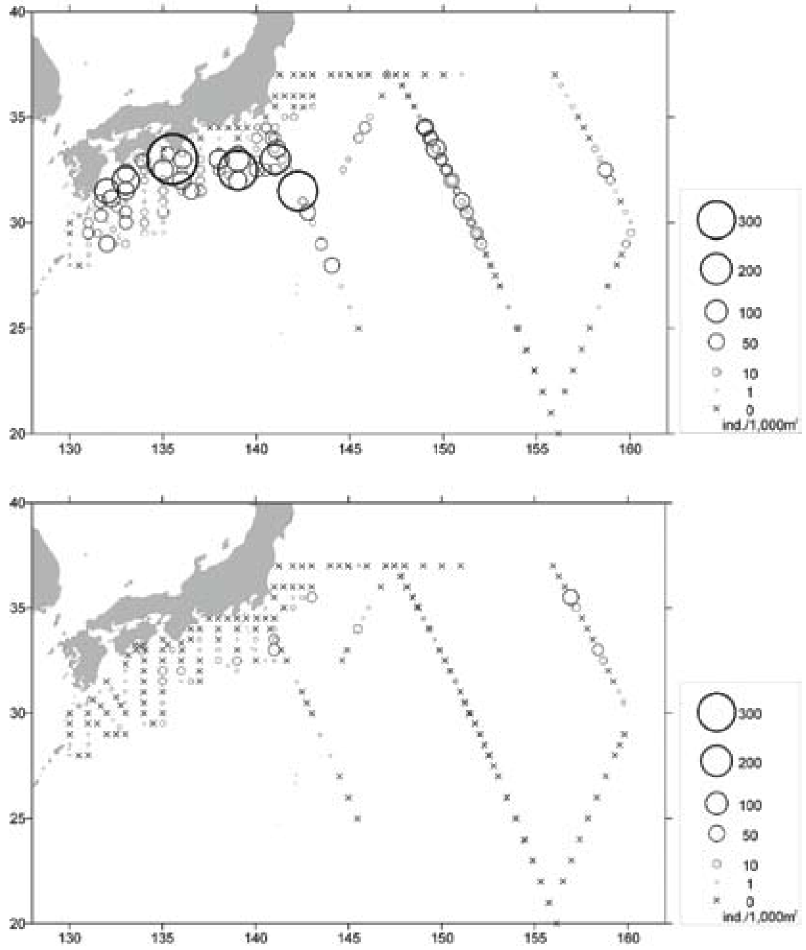

[Figure KU-25] Distributions of larval and juvenile Pacific saury *Cololabis saira* in 2004. Larvae (upper panel) and juveniles (lower panel) are classified by 25 mm in knob length. The data were collected from egg and larvae of Pacific saury research coordinated by the Fisheries Agency of Japan (Oozeki et al. 2007b).

References

Adler, R.F., Huffman, G.J., Chang, A., Ferraro, R., Xie, P.P., Janowiak, J., Rudolf, B., Schneider, U., Curtis, S., Bolvin, D., Gruber, A., Susskind, J., Arkin, P., Nelkin, E. 2003. The version-2 Global Precipitation Climatology Project (GPCP) monthly precipitation analysis (1979-present). Journal of Hydrometeorology 4: 1147–1167.

Akitmoto, K., Awaji, T., Imasato, N. 1991. Kuroshio path variation south of Japan. 1. Barotropic inflow-outflow model. Journal of Geophysical Research 96: 2549-2560.

Akitmoto, K., Masuda, S., Awaji, T. 1997. Kuroshio path variation south of Japan: Stability of the paths in a multiple equilibrium regime. Journal of Oceanography 53: 129-142.

Anonymous. 2006-2008. Annual meeting report of egg and larval survey of small pelagic fish off the Pacific coast of Japan. Fisheries Research Agency of Japan No. 26–No. 28 (in Japanese).

Anonymous. 2009. Marine fisheries stock assessment and evaluation for Japanese waters (fiscal year 2008/2009). Fisheries Agency and Fisheries Research Agency of Japan 1553 pp. (in Japanese).

Barange, M., Coetzee, J., Takasuka, A., Hill, K., Gutierreze, M., Oozeki, Y., van der Lingen, C., Agostini, V. 2009. Habitat expansion and contraction in anchovy and sardine populations. Progress in Oceanography 83: 251-260.

Ceballos, L.I., Di Lorenzo, E., Hoyos, C.D., Schneider, N., Taguchi, B. 2009. North Pacific Gyre Oscillation synchronizes climate fluctuations in the eastern and western boundary systems. Journal of Climate 22: 5163-5174.

Checkley, D., Ayon, P., Baumgartner, T.R., Bernal, M., Coetzee, J.C., Emmett, R., Guevara, R., Hutching, L., Ibaibarriaga, L., Nakata, H., Oozeki, Y., Planque, B., Schweigert, J., Stratoudaki, Y., Van der Lingen, C.D. 2009. Habitats, pp. 12-44, In Checkley, D., Alheit, J., Oozeki, Y., Roy, C. (eds.), Climate change and small pelagic fish, Cambridge University Press, London.

Chiba, S., Aita, M.N., Tadokoro, K., Saino, T., Sugisaki, H., Nakata, K. 2008. From climate regime shifts to lower-tropic level phenology: Synthesis of recent progress in retrospective studies of the western North Pacific. Progress in Oceanography 77: 112-126.

Deser, C., Alexander, M.A., Timlin, M.S. 1999. Evidence for a wind-driven intensification of the Kuroshio current extension from the 1970s to 1980s. Journal of Climate 12: 1697-1706.

Dore, J.E., Lukas, R., Sadler, D.W., Karl, D.M. 2003. Climate-driven changes to the atmospheric CO2 sink in the subtropical North Pacific Ocean. Nature 424: 754-757.

Fuentes-Yaco, C., Koeller, P.A., Sathyendranath, S., Platt, T. 2007. Shrimp (*Pandalus borealis*) growth and timing of the spring phytoplankton bloom on the Newfoundland-Labrador Shelf. Fisheries Oceanography 16: 116-129.

Hanawa, K., Kamada, J. 2001. Variability of core layer temperature (CLT) of the North Pacific Subtropical Mode Water. Geophysical Research Letters 28: 2229-2232.

Honda, M., Inoue, J., Yamane, S. 2009. Influence of low Arctic sea-ice minima on anomalously cold Eurasian winters. Geophysical Research Letters 36: L08707, doi:10.1029/2008GL037079.

Honda, M., Yamane, S., Nakamura, H. 2005. Impacts of the Aleutian-Icelandic low seesaw on surface climate during the twentieth century. Journal of Climate 18: 2793-2802.

Ishida, M., Kikuchi, H. 1992. Monthly egg productions of the Japanese sardine, anchovy, and mackerels of the southern coast of Japan by egg censuses: January 1989 through December, 1990. Japan Fisheries Agency, 86 pp. (in Japanese with English abstract).

Kalnay, E., Kanamitsu, M., Kistler, R., Collins, W., Deaven, D., Gandin, L., Iredell, M., Saha, S., White, G., Woollen, J., Zhu, Y., Leetmaa, A., Reynolds, R., Chelliah, M., Ebisuzaki, W., Higgins, W., Janowiak, J., Mo, K., Ropelewski, C., Wang, J., Jenne, R., Joseph, D. 1996. The NCEP/NCAR 40-Year Reanalysis Project. Bulletin of the American Meteorological Society 77: 437-471.

Kawabata, A., Nakagami, M., Suyama, S. 2008a. Distribution of juvenile Japanese sardine in the recent low biomass level: using the feeding ground off the Kuril Islands. 1c_024. In Proceedings of 5th World Fisheries Congress, TerraPub, Tokyo.

Kawabata, A., Nakagami, M., Suyama, S., Nishida, H., Watanabe, C. 2008b. Distribution and migration in relation to the recent increase of biomass of age-1 and older spotted mackerel in the western North Pacific. Fisheries Biology and Oceanography in the Kuroshio 9: 61-66 (in Japanese).

Kawabe, M., 1995. Variations of current path, velocity, and volume transport of the Kuroshio in relation with the large meander. Journal of Physical Oceanography 25: 3103-3117.

Kawai, H. 1969. Statistical estimation of isotherms indicative of Kuroshio axis. Deep-Sea Research 16 (supplement): 109-115.

Kawasaki, T. 1966. Structure of the Pacific population of the mackerel. Bulletin of Tokai Regional Fisheries Research Laboratory 47: 1-34 (in Japanese).

Kikuchi, H., Konishi, Y. 1990. Monthly egg productions of the Japanese sardine, anchovy, and mackerels of the southern coast of Japan by egg censuses: January 1987 through December 1988. Japan Fisheries Agency, 72 pp. (in Japanese with English abstract).

Kubota, H., Oozeki, Y., Ishida, M., Konishi, M., Goto, T., Zenitani, H., Kimura, R. 1999. Distributions of eggs and larvae of Japanese sardine, Japanese anchovy, mackerels, round herring, jack mackerel and Japanese common squid in the waters around Japan, 1994 through 1996. National Research Institute of Fisheries Science, Yokohama, 352 pp. (in Japanese with English abstract).

Lee, E.-J., Jhun, J.G., Park, C.-K. 2005. Remote connection of the Northeast Asian summer rainfall variation revealed by a newly defined monsoon index. Journal of Climate 18: 4381-4393.

Levitus, S., Antonov, I., Boyer, T.P., Stephens, C. 2000. Warming of world ocean. Science 287: 2225-2229.

Limsakul, A., Saino, T., Midorikawa, T., Goes, J.I. 2001. Temporal variations in lower trophic level biological environments in the northwestern North Pacific Subtropical Gyre from 1950 to 1997. Progress in Oceanography 49: 129-149.

Lukas, R. 2001. Freshening of the upper thermocline in the North Pacific subtropical gyre associated with decadal changes of rainfall. Geophysical Research Letters 28: 3485-3488.

Meguro, K. 2008. Eggs and larvae of Chub mackerel *Scomber japonicus* and spotted mackerel *Scomber australasicus* taken by artificial fertilization. Bulletin of the Chiba Prefectural Fisheries Research Center 1: 33-43 (in Japanese).

Miller, A.J., Cayan, D.R., White, W.B. 1998. A westward-intensified decadal change in the North Pacific thermocline and gyre-scale circulation. Journal of Climate 11: 3112-3127.

Minobe, S., Nakanowatari, T. 2002. Global structure of bidecadal precipitation variability in boreal winter. Geophysical Research Letters 29: 1396, doi:10.1029/2001GL014447.

Mori, K., Kuroda, K., Konishi, Y. 1988. Monthly egg productions of the Japanese sardine, anchovy, and mackerels off the southern coast of Japan by egg censuses: January 1978 through December 1986. Bulletin of Tokai Regional Fisheries Research Laboratory, Tokyo, 321 pp.

Murayama, T., Mitani, I., Aoki, I. 1995. Estimation of the spawning period of the Pacific mackerel *Scomber japonicus* based on the changes in gonad index and the ovarian histology. Bulletin of the Japanese Society of Fisheries Oceanography 59: 11-17 (in Japanese).

Nagai, N. 2004. Middle and long-term variations of marine plankton along JMA's 137°E hydrographic section. Weather Service Bulletin 71 (Suppl.): 17-26 (in Japanese).

Nakamura, H., Izume, T., Sampe, T. 2002. Interannual and decadal modulations recently observed in the Pacific storm track activity and East Asian winter monsoon. Journal of Climate 15: 1855-1874.

Nakanowatari, T., Minobe, S. 2005. Moisture balance for bidecadal variability of wintertime precipitation in the North Pacific using NCEP/NCAR reanalysis. Journal of the Meteorological Society of Japan 83: 453-469.

Nakata K., Hidaka, K. 2003. Decadal-scale variability in the Kuroshio marine ecosystem in winter. Fisheries Oceanography 12: 234-244.

Nakata K., Koyama, S. 2003. Interannual changes of the winter to early spring biomass and composition of mesozooplankton in the Kuroshio region in relation to climatic factors. Journal of Oceanography 59: 225-234.

Nonaka, M., Nakamura, H., Tanimoto, Y., Kagimoto, T., Sasaki, H. 2006. Decadal variability in the Kuroshio-Oyashio Extension simulated in an eddy-resolving OGCM. Journal of Climate 19: 1970-1989.

Odate, S. 1961. Study on the larvae of the fishes in the north-eastern sea area along the Pacific coast of Japan. Part 1. Mackerel, *Pneumatophorus japonicus* (Houttuyn). Bulletin of the Tohoku Regional Fisheries Research Laboratory 19: 98-108 (in Japanese).

Oozeki, Y., Takasuka, A., Kubota, H., Barange, M. 2007a. Characterizing spawning habitats of Japanese sardine, *Sardinops melanostictus*, Japanese anchovy, *Engraulis japonicus*, and Pacific round herring, *Etrumeus teres*, in the Northwestern Pacific. California Cooperative Oceanic Fisheries Investigations Report 48: 191-203.

Oozeki, Y., Kubota, H., Takasuka, A., Watanabe, T., Yasuda, I., Itoh, S., Moku, M., Yoshimura, T. 2007b. Larval distribution of Pacific saury in the Kuroshio recirculation region. Annual Report of the Research Meeting on Saury Resources 55: 281-283 (in Japanese).

Overland, J.E., Salo, S., Adams, J.M. 1999. Salinity signature of the Pacific Decadal Oscillation, Geophysical Research Letters 26: 1337-1340.

Qiu, B., Chen, S. 2005. Variability of the Kuroshio Extension jet, recirculation gyre, and mesoscale eddies on decadal time scales. Journal of Physical Oceanography 35: 2090-2103.

Reiss, C.S., Checkley, D.M. Jr., Bograd, S.J. 2008. Remotely sensed spawning habitat of Pacific sardine (*Sardinops sagax*) and Northern anchovy (*Engraulis mordax*) within the California Current. Fisheries Oceanography 17: 126-136.

Seager R., Kushnir, Y., Naik, N.H., Cane, M.A., Miller, J. 2001. Wind-driven shifts in the latitude of the Kuroshio-Oyashio extension and generation of SST anomalies on decadal timescales. Journal of Climate 14: 4149-4165.

Shimizu T., Moriyama, E., Goto, H., Sasano, D., Aoyama, M. 2004. Seasonal variations and long-term trends of chemical and biological parameters along PN-line. Weather Service Bulletin 71 (Suppl.): 35-44 (in Japanese).

Sugimoto, T., Tadokoro, K. 1998. Interdecadal variations of plankton biomass and physical environment in the North Pacific. Fisheries Oceanography 7: 289-299.

Tadokoro K., Ono, T., Yasuda, I., Osafune, S., Shiomoto, A., Sugisaki, H. 2009. Possible mechanism of decadal-scale variation in PO4 comcentration in the wetern North Pacific. Geophysical Research Letters 36: 8, doi: 10. 1029/2009GL037327

Taguchi, B., Xie, S.-P., Schneider, N., Nonaka, M., Sasaki, H., Sasai, Y. 2007. Decadal variability of the Kuroshio Extension: Observations and an eddy-resolving model hindcast. Journal of Climate 20: 2357–2377.

Takasuka, A., Oozeki, Y., Kubota, H. 2008. Multi-species regime shifts reflected in spawning temperature optima of small pelagic fish in the western North Pacific. Marine Ecology Progress Series 360: 211-217.

Trenberth, K.E., Hurrell, J.W. 1994. Decadal atmosphere-ocean variations in the Pacific. Climate Dynamics 9: 303-319.

Usami, S. 1973. Ecological studies of life pattern of the Japanese mackerel, *Scomber japonicus* Houttuyn: on the adult of the Pacific subpopulation. Bulletin of Tokai Regional Fisheries Research Laboratory 76: 71-178 (in Japanese).

Walker, G.T., Bliss, E.W. 1932. World weather V. Memoirs of the Royal Meteorological Society 4: 53-84.

Wallace, J.M., Gutzler, D.S. 1981. Teleconnections in the geopotential height field during the Northern Hemisphere winter. Monthly Weather Review 109: 784-812.

Wang, B., Wu, R., Fu, X. 2000. Pacific-East Asian teleconnection: How does ENSO affect East Asian climate? Journal of Climate 13: 1517-1536.

Wang, B., Wu, Z., Li, J., Liu, J., Chang, C.-P., Ding, Y., Wu, G. 2008. How to measure the strength of the East Asian summer monsoon. Journal of Climate 21: 4449-4463.

Watanabe, Y., Kurita, Y., Noto, M., Oozeki, Y., Kitagawa, D. 2003. Growth and survival processes of Pacific saury *Cololabis saira* in the Kuroshio-Oyashio transitional waters. Journal of Oceanography 59: 403-414.

Watanabe, T. 1970. Morphology and ecology of early stages of life in Japanese common mackerel, *Scomber japonicus* Houttuyn, with special reference to fluctuation of population. Bulletin of Tokai Regional Fisheries Research Laboratory 62: 1-283 (in Japanese).

Watanabe, C., Hanai, T., Meguro, K., Ogino, R., Kubota, Y., Kimura, R. 1999. Spawning biomass estimates of chub mackerel *Scomber japonicus* of Pacific subpopulation off central Japan by a daily egg production method. Nippon Suisan Gakkaishi 65: 695-702 (in Japanese).

Watanabe, C., Nishida, H. 2002. Development of assessment techniques for pelagic fish stocks: applications of daily egg production method and pelagic trawl in the northwestern Pacific Ocean. Fisheries Science 68: 97-100.

Xie, S.-P., Hu, K., Hafner, J., Tokinaga, H., Du, Y., Huang, G., Sampe, T. 2009. Indian Ocean capacitor effect on Indo–Western Pacific climate during the summer following El Niño. Journal of Climate 22: 730-747.

Yasuda, T., Kitamura, Y. 2003. Long-term variability of North Pacific Subtropical Mode Water in response to spin-up of the subtropical gyre. Journal of Oceanography 59: 279-290.

Zenitani, H., Ishida, M., Konishi, Y., Goto, T., Watanabe, Y., Kimura, R. 1995. Distributions of eggs and larvae of Japanese sardine, Japanese anchovy, mackerels, round herring, Japanese horse mackerel and Japanese common squid in the waters around Japan, 1991 through 1993. Japan Fisheries Agency, 368 p.